

Second order viscous corrections to the harmonic spectrum in heavy ion collisions

D. Teaney^{*} and L. Yan[†]

*Department of Physics & Astronomy,
Stony Brook University, Stony Brook, NY 11794, USA*

Abstract

We calculate the second order viscous correction to the kinetic distribution, $\delta f_{(2)}$, and use this result in a hydrodynamic simulation of heavy ion collisions to determine the complete second order correction to the harmonic spectrum, v_n . At leading order in a conformal fluid, the first viscous correction is determined by one scalar function, χ_{0p} . One moment of this scalar function is constrained by the shear viscosity. At second order in a conformal fluid, we find that $\delta f(\mathbf{p})$ can be characterized two scalar functions of momentum, χ_{1p} and χ_{2p} . The momentum dependence of these functions is largely determined by the kinematics of the streaming operator. Again, one moment of these functions is constrained by the parameters of second order hydrodynamics, τ_π and λ_1 . The effect of $\delta f_{(2)}$ on the integrated flow is small (up to v_4), but is quite important for the higher harmonics at modestly-large p_T . Generally, $\delta f_{(2)}$ increases the value of v_n at a given p_T , and is most important in small systems.

^{*} derek.teaney@stonybrook.edu

[†] li.yan@stonybrook.edu

I. INTRODUCTION

Motivated by the wealth of data on collective flow in heavy ion collisions, hydrodynamic simulations of these ultra-relativistic events have steadily improved. Today, event by event viscous hydrodynamic simulations reproduce the elliptic flow, the triangular flow, the higher harmonic flows, and the correlations between the flow harmonics and event plane angles [1]. The overall agreement with the data on this rich variety of observables constrains the shear viscosity of the QGP close to transition region. Because this success, there is a current need to precisely quantify the systematic uncertainties in these simulations and the corresponding uncertainty in the extracted shear viscosity of the QGP [2]. This paper will address this need by computing the second order corrections to the thermal distribution function [3, 4] and by using these results to simulate the observed harmonic spectrum.

Since the nucleus is not vastly larger than the mean free path, an important advance in hydrodynamic simulations was the inclusion of viscous corrections to the hydrodynamic equations of motion at first and second order in the gradient expansion. In particular Baier, Romatschke, Son, Starinets, Stephanov (BRSSS) determined the possible tensor forms that arise in the constituent relation of a conformal fluid at second order [3]. These equations are currently used in practically all viscous simulations of heavy ion collisions. It is satisfying that the gradient expansion, which underlies the hydrodynamic approach, seems to converge [5], and seems to converge to the measured flow [1]. However, all simulations of heavy ion collisions make additional kinetic assumptions about the fluid at freezeout when computing the particle spectra [6]. Indeed, the phase space distribution of a viscous fluid $f_{\mathbf{p}}(X)$ is modified from its equilibrium form, $n_{\mathbf{p}}(X)$, by corrections at first and second order, $\delta f_{\mathbf{p}} = \delta f_{(1)} + \delta f_{(2)}$. Currently, all simulations of heavy ion collisions compute the viscous corrections to the distribution function at first order, while using second order corrections to the hydrodynamic equations of motion. The goal of this work is to remedy this inconsistency by computing viscous corrections to the distribution function to second order. Then, this second order correction is used to compute the harmonic spectrum, $v_n(p_T)$. As expected [7], these corrections are modest for small harmonic numbers, n , and small p_T , but grow both with n and p_T .

To compute the viscous corrections to the phase space distribution we will analyze kinetic theory of a conformal gas close to equilibrium in a relaxation time approximation. This extreme idealization is still useful for several reasons. First, a similar equilibrium analysis of QCD kinetic theory was used to determine the second order transport coefficients to leading order in α_s [4]. This analysis (which will be discussed further below) makes clear that the details of the collision integral hardly matter in determining the second order transport coefficients. Indeed, we will see that the structure of the second order viscous correction $\delta f_{(2)}$ is largely determined by the kinematics of free streaming, rather than the details of the collision integral. Thus, an analysis based on a relaxation time approximation is an easy way to reliably estimate the size of such second order corrections in heavy ion collisions. Second, the overall normalization of $\delta f_{(2)}$ is constrained by the second order transport coefficients τ_π and λ_1 , in much the same way that the shear viscosity constrains the normalization of $\delta f_{(1)}$. These constraints allow us to make a good estimate of the form of viscous corrections at second order for a realistic non-conformal fluid.

With this functional form we study the effect of $\delta f_{(2)}$ on the harmonic spectrum in heavy ion collisions. In Section II we outline how $\delta f_{(2)}$ is computed in kinetic theory. Then, in

Section III we discuss the practical implementation of this formula in a hydrodynamic code used to simulate heavy ion collisions. These results are used to simulate the linear response to a given deformation, ϵ_n . The linear response is largely responsible for determining the v_n in central collisions. In non-central collisions the linear response *and* the quadratic response determine the harmonic flow and its correlations [1, 8–11], but the quadratic response will not be discussed in this initial study. Finally, we will summarize the effects of $\delta f_{(2)}$ in Section IV.

II. 2ND ORDER CORRECTIONS TO THE PHASE SPACE DISTRIBUTION

A. Notation

Throughout the paper we will work with the metric $\eta^{\mu\nu} = (-, +, +, +)$, and $d = 4$ denotes the number of space-time dimensions. Capital letters P, X denote four vectors, while lower case letters \mathbf{p}, \mathbf{x} denote three vectors in the rest frame.

We are expanding around a fluid in equilibrium with energy density, pressure, and flow velocity equal to $e(X)$, $\mathcal{P}(X)$, and $U^\mu(X)$ respectively where $U^\mu U_\mu = -1$. Thus, the rest frame projector is $\Delta^{\mu\nu} = g^{\mu\nu} + U^\mu U^\nu$, and the spatial derivatives and temporal derivatives are $\nabla^\mu = \Delta^{\mu\nu} \partial_\nu$ and $D = U^\mu \partial_\mu$, respectively. Finally bracketed tensors are rendered symmetric-traceless and orthogonal to U^μ ,

$$\langle A^{\mu\nu} \rangle = \frac{1}{2} \Delta^\mu_\rho \Delta^\nu_\sigma (A^{\rho\sigma} + A^{\sigma\rho}) - \frac{1}{(d-1)} \Delta^{\mu\nu} \Delta_{\rho\sigma} A^{\rho\sigma}. \quad (2.1)$$

Such tensors transform irreducibly under rotation in the local rest frame. A more elaborate example using $\sigma_{\mu\nu} = 2 \langle \nabla_\mu U_\nu \rangle$ which appears in the algebra below is

$$\begin{aligned} \{\sigma_{\mu_1\mu_2}\sigma_{\mu_3\mu_4}\}_{\text{sym}} &= \langle \sigma_{\mu_1\mu_2}\sigma_{\mu_3\mu_4} \rangle + \frac{4}{d+3} \{\Delta_{\mu_1\mu_2} \langle \sigma_{\mu_3}^\lambda \sigma_{\mu_4\lambda} \rangle\}_{\text{sym}} \\ &\quad + \frac{2}{(d-1)(d+1)} \{\Delta_{\mu_1\mu_2} \Delta_{\mu_3\mu_4}\}_{\text{sym}} \sigma^2, \end{aligned} \quad (2.2)$$

where the symmetrized spatial tensor is denoted with curly brackets:

$$\{\sigma_{\mu_1\mu_2}\sigma_{\mu_3\mu_4}\}_{\text{sym}} = \frac{1}{3} [\sigma_{\mu_1\mu_2}\sigma_{\mu_3\mu_4} + \sigma_{\mu_1\mu_3}\sigma_{\mu_2\mu_4} + \sigma_{\mu_1\mu_4}\sigma_{\mu_2\mu_3}]. \quad (2.3)$$

The equilibrium distribution function is $n_{\mathbf{p}} \equiv n(-P \cdot U(X)/T(X))$ where $n(z) = 1/(e^z \mp 1)$, and $f_{\mathbf{p}}(X)$ denotes the full non-equilibrium distribution. The rest frame integrals are abbreviated $\int_{\mathbf{p}} \equiv \int d^{d-1}p/(2\pi)^{d-1}$ and primes (such as $n'_{\mathbf{p}}$) denote derivatives with respect to $-P \cdot U/T$, so that $n'_{\mathbf{p}} = -n_{\mathbf{p}}(1 \pm n_{\mathbf{p}})$. The energy and squared three momentum in the rest frame are, $E_{\mathbf{p}} = -P \cdot U$ and $p^2 = P^\mu P^\nu \Delta_{\mu\nu}$, respectively.

B. Hydrodynamics

In evaluating $\delta f_{(2)}$ to second order we will need the hydrodynamic equations of motion. In the Landau frame these equations read

$$T^{\mu\nu} = eU^\mu U^\nu + \mathcal{P}\Delta^{\mu\nu} + \pi^{\mu\nu}, \quad \partial_\mu T^{\mu\nu} = 0, \quad (2.4)$$

where $\pi^{\mu\nu}$ is the viscous correction to the stress tensor. Throughout this analysis we are working with a conformal fluid, and consequently the bulk viscosity is zero $\zeta = 0$. For a conformal fluid the possible tensor forms of the gradient expansion for $\pi^{\mu\nu}$ through second order were established by BRSSS

$$\pi^{\mu\nu} = \pi_{(1)}^{\mu\nu} + \pi_{(2)}^{\mu\nu} + \dots = -\eta\sigma^{\mu\nu} + \eta\tau_\pi \left[\langle D\sigma^{\mu\nu} \rangle + \frac{1}{d-1}\sigma^{\mu\nu}\partial \cdot U \right] + \lambda_1 \langle \sigma^\mu{}_\lambda \sigma^{\nu\lambda} \rangle + \lambda_2 \langle \sigma^\mu{}_\lambda \Omega^{\nu\lambda} \rangle + \lambda_3 \langle \Omega^\mu{}_\lambda \Omega^{\nu\lambda} \rangle + \dots, \quad (2.5)$$

where $-\eta\sigma^{\mu\nu} = -2\eta \langle \nabla^\mu U^\nu \rangle$ is the first order term, and the vorticity tensor is

$$\Omega^{\mu\nu} = \frac{1}{2} \Delta^{\mu\alpha} \Delta^{\nu\beta} (\partial_\alpha U_\beta - \partial_\beta U_\alpha). \quad (2.6)$$

The ellipses in Eq. (2.5) denote terms third order in the gradients. Using these equations of motion, the time derivatives of the energy density and flow velocity can be determined from the spatial gradients of these fields

$$De = -(e + \mathcal{P})\nabla \cdot U + \frac{\eta}{2}\sigma_{\mu\nu}\sigma^{\mu\nu} + \dots, \quad (2.7a)$$

$$DU_\mu = -\frac{\Delta_\mu \mathcal{P}}{e + \mathcal{P}} - \frac{\Delta_{\mu\lambda_2} \partial_{\lambda_1} \pi^{\lambda_1\lambda_2}}{e + \mathcal{P}}, \quad (2.7b)$$

$$= -\frac{\nabla_\alpha \mathcal{P}}{e + \mathcal{P}} + \frac{\eta}{e + \mathcal{P}} [(d-2) \langle \sigma_{\mu\lambda} \nabla^\lambda \ln T \rangle + \langle \nabla_\lambda \sigma^\lambda{}_\mu \rangle] + \dots. \quad (2.7c)$$

In passing from Eq. (2.7b) to Eq. (2.7c) we have used the first order expression for $\pi^{\mu\nu} = -\eta\sigma^{\mu\nu}$, the conformal temperature dependence of $\eta \propto T^{d-1}$, and the lowest order equations of motion.

In hydrodynamic simulations of heavy ion collisions the static form of the constituent relation Eq. (2.5) is not used. Rather, this equation is rewritten as a dynamical equation for $\pi_{\mu\nu}$ which is evolved numerically [3]

$$\pi^{\mu\nu} = -\eta\sigma^{\mu\nu} - \tau_\pi \left[\langle D\pi^{\mu\nu} \rangle + \frac{d}{d-1}\pi^{\mu\nu}\nabla \cdot U \right] + \frac{\lambda_1}{\eta^2} \langle \pi^\mu{}_\lambda \pi^{\nu\lambda} \rangle - \frac{\lambda_2}{\eta} \langle \pi^\mu{}_\lambda \Omega^{\nu\lambda} \rangle + \lambda_3 \langle \Omega^\mu{}_\lambda \Omega^{\nu\lambda} \rangle. \quad (2.8)$$

Similarly, when constructing δf at first and second order we will systematically replace $\sigma_{\mu\nu}$ with $-\pi_{\mu\nu}/\eta$. For fluids with an underlying kinetic description, the transport coefficients are additionally constrained, with $\lambda_3 = 0$ and $\lambda_2 = -2\eta\tau_\pi$ [4], and these relations used in the simulation. The appropriate values for λ_1 and $\eta\tau_\pi$ will be discussed below.

C. Kinetics

To determine the viscous corrections to the distribution function we will solve the kinetic equations in a relaxation time approximation through second order in the gradient expansion

$$f_{\mathbf{p}} \equiv n_{\mathbf{p}} + \delta f_{\mathbf{p}} = n_{\mathbf{p}} + \delta f_{(1)} + \delta f_{(2)} + \dots. \quad (2.9)$$

In a relaxation time approximation the Boltzmann equation reads

$$P^\mu \partial_\mu f_{\mathbf{p}}(X) = -\frac{T^2}{\mathcal{C}_p} [f_{\mathbf{p}}(X) - n(-P \cdot U_*(X)/T_*(X))] , \quad (2.10)$$

where the dimensionless coefficient \mathcal{C}_p is related to the canonically defined momentum dependent relaxation time

$$\mathcal{C}_p = T^2 \frac{\tau_R(E_p)}{E_p} . \quad (2.11)$$

Following Ref. [7], we will parametrize the momentum dependence of the relaxation time as a simple power law

$$\tau_R \propto E_{\mathbf{p}}^{1-\alpha} , \quad (2.12)$$

with α between zero and one. As we will see below, $\alpha = 0$ gives a first order a viscous correction which grows quadratically with momentum (which is known as the quadratic ansatz), while $\alpha = 1$ gives a first order viscous correction which grows linearly with momentum (and is known as the linear ansatz).

At leading order, the parameters T_* and U_*^μ which appear in the kinetic equation are equal to the Landau matched temperature and flow velocity, T and U^μ . However, starting at second order T_* and U_*^μ will differ from T and U^μ by squares of gradients:

$$T_*(X) \equiv T(X) + \delta T_*(X) , \quad (2.13a)$$

$$U_*^\mu(X) \equiv U^\mu(X) + \delta U_*^\mu(X) . \quad (2.13b)$$

δT_* and δU_*^μ will be determined at each order by the Landau matching condition:

$$T^{\mu\nu} U_\nu = e U^\mu .$$

Expanding $n(-P \cdot U_*/T_*)$ we have

$$n_{\mathbf{p}}^* \equiv n_{\mathbf{p}} + \delta n_{\mathbf{p}}^* \quad \delta n_{\mathbf{p}}^* = n'_{\mathbf{p}} \left[-\frac{P \cdot \delta U_*}{T} - E_p \frac{\delta T_*}{T^2} \right] + \dots , \quad (2.14)$$

where we have used an obvious notation, $n_{\mathbf{p}}^* \equiv n(-P \cdot U_*/T_*)$ and $n_{\mathbf{p}} \equiv n(-P \cdot U/T)$.

Then to determine δf we substitute the expansion (Eq. (2.9)) into the relaxation time equation and equate orders. In doing so we use the hydrodynamic equations of motion through second order to write time derivatives of $T(X)$ and $U^\mu(X)$ in terms of spatial gradients of these fields. For instance, using the equations of motion Eq. (2.7) and the thermodynamic identities

$$c_v = \frac{de}{dT} , \quad \frac{1}{T(e + \mathcal{P})} d\mathcal{P} + d\left(\frac{1}{T}\right) = 0 , \quad c_s^2 = \frac{e + \mathcal{P}}{T c_v} , \quad (2.15)$$

and the relations $p^2 = E_p^2$ and $c_s^2 = 1/(d-1)$ of a conformal gas, we have

$$P^\mu \partial_\mu n_{\mathbf{p}} = -n'_{\mathbf{p}} \frac{p^\mu p^\nu}{2T} \sigma_{\mu\nu} - \frac{n'_{\mathbf{p}}}{(e+p)T} \left[-E_p P^{\mu_1} \Delta_{\mu_1 \mu_2} \partial_\lambda \pi^{\lambda \mu_2} + \frac{1}{2} E_p^2 c_s^2 \eta \sigma^2 \right] + \dots \quad (2.16)$$

The term linearly proportional to $\sigma_{\mu\nu}$ is ultimately responsible for the shear viscosity, while the nonlinear terms contribute to $\delta f_{(2)}$.

With this discussion, we find that the δf is determined by the hierarchy of equations:

$$\delta f_{(1)}^\sigma = \mathcal{C}_p n'_p \frac{P^\mu P^\nu \sigma_{\mu\nu}}{2T^3}, \quad (2.17)$$

and

$$\delta f_{(2)}^\sigma = \delta n_{\mathbf{p}}^* + \frac{\mathcal{C}_p n'_p}{(e+p)T^3} \left[-E_p P^{\mu_1} \Delta_{\mu_1 \mu_2} \partial_\lambda \pi^{\lambda \mu_2} + \frac{1}{2} E_p^2 c_s^2 \eta \sigma^2 \right] - \frac{\mathcal{C}_p}{T^2} P^\mu \partial_\mu \delta f_{(1)}^\sigma. \quad (2.18)$$

Straightforward algebra uses the equations of motion to decompose $\delta f_{(2)}$ into irreducible tensors, and determines the final form of $\delta f_{(1)}^\sigma$ and $\delta f_{(2)}^\sigma$ (see Appendix A).

We have put a superscript σ in $f_{(1)}^\sigma$ and $\delta f_{(2)}^\sigma$ to indicate that that we are using $\sigma_{\mu\nu}$ rather than $\pi_{\mu\nu}$ in these equations. In realistic hydrodynamic simulations of heavy ion collisions $\pi_{\mu\nu}$ is treated as a dynamic variable, and $-\eta\sigma_{\mu\nu}$ is systematically replaced by $\pi_{\mu\nu}$. This yields the following reparametrization of δf

$$\delta f_{(1)} = -\frac{1}{2} \mathcal{C}_p n'_p \frac{P^\mu P^\nu}{\eta T^3} \pi_{\mu\nu}, \quad (2.19a)$$

$$\delta f_{(2)} = \delta f_{(2)}^\sigma + \frac{1}{2} \mathcal{C}_p n'_p \frac{P^\mu P^\nu}{\eta T^3} [\pi_{\mu\nu} + \eta \sigma_{\mu\nu}], \quad (2.19b)$$

where we have replaced $\sigma_{\mu\nu}$ with $-\pi_{\mu\nu}/\eta$ in the first order result, and appended the difference between these two tensors to the second order result so that, $\delta f_{(1)} + \delta f_{(2)} = \delta f_{(1)}^\sigma + \delta f_{(2)}^\sigma$ up to third order terms.

To record the result for $\delta f_{(2)}$, we first review the familiar first order case. At first order, $\delta f_{(1)}$ is described by a dimensionless scalar function $\chi_{0p}(E_p/T)$

$$\delta f_1 = \chi_{0p} \frac{P^{\mu_1} P^{\mu_2}}{\eta T^3} \pi_{\mu_1 \mu_2}, \quad (2.20)$$

which has been extensively studied in the literature, and determines the shear viscosity [7]. In the relaxation time approximation this function is related to the relaxation time

$$\chi_{0p} = -\frac{1}{2} \mathcal{C}_p n'_p. \quad (2.21)$$

One moment of this function is constrained by the shear viscosity. Indeed, from the defining relation

$$\pi^{\mu\nu} = \int_{\mathbf{p}} \frac{P^\mu P^\nu}{P^0} \delta f_{\mathbf{p}}, \quad (2.22)$$

we determine the shear viscosity

$$\eta = \frac{2}{(d-1)(d+1)T^3} \int_{\mathbf{p}} \frac{p^4}{E_p} \chi_{0p}, \quad (2.23)$$

and a constraint on $\delta f_{(2)}$

$$0 = \int_{\mathbf{p}} \frac{P^\mu P^\nu}{P^0} \delta f_{(2)}. \quad (2.24)$$

This constraint reflects the reparametrization of $\sigma^{\mu\nu}$ in the first order $\delta f_{(1)}$ with $\pi^{\mu\nu}$. For later use and comparison, we note that the enthalpy is

$$(e + \mathcal{P}) = \frac{-1}{(d-1)T} \int_{\mathbf{p}} n'_p p^2, \quad (2.25)$$

which can be obtained by comparing the stress tensor from kinetic theory for small fluid velocities (*i.e.* $U^\mu \simeq (1, \mathbf{v})$ with $\mathbf{v} \ll 1$) to ideal hydrodynamics, $T^{0i} \simeq (e + \mathcal{P})v^i$ [12].

At second order the function $\delta f_{(2)}$ is described by two dimensionless scalar functions χ_{1p} and χ_{2p}

$$\chi_{1p} = -\frac{1}{2} \mathcal{C}_p \chi'_{0p}, \quad (2.26)$$

$$\chi_{2p} = \mathcal{C}_p \chi_{0p}. \quad (2.27)$$

Two moments of these scalar functions are constrained by the second order transport coefficients $\eta\tau_\pi$ and λ_1

$$\lambda_1 + \eta\tau_\pi = \frac{8}{(d-1)(d+1)(d+3)T^6} \int_{\mathbf{p}} \chi_{1p} \frac{p^6}{E_p}, \quad (2.28)$$

$$\eta\tau_\pi = \frac{2}{(d-1)(d+1)T^5} \int_{\mathbf{p}} \chi_{2p} p^4. \quad (2.29)$$

Then the functional form of $\delta f_{(2)}$ is

$$\begin{aligned} \delta f_{(2)} = & \frac{\chi_{1p}}{\eta^2} \frac{P^{\mu_1} P^{\mu_2} P^{\mu_3} P^{\mu_4}}{T^6} \langle \pi_{\mu_1 \mu_2} \pi_{\mu_3 \mu_4} \rangle + \frac{\chi_{2p}}{\eta} \frac{P^{\mu_1} P^{\mu_2} P^{\mu_3}}{T^5} [(d+2) \langle \pi_{\mu_1 \mu_2} \nabla_{\mu_3} \ln T \rangle - \langle \nabla_{\mu_1} \pi_{\mu_2 \mu_3} \rangle] \\ & + \frac{\xi_{1p}}{\eta^2} \frac{P^{\mu_2} P^{\mu_1}}{T^4} \langle \pi_{\mu_2}^\lambda \pi_{\mu_1 \lambda} \rangle + \frac{\xi_{2p}}{\eta} \frac{P^{\mu_2} P^{\mu_1}}{T^3} [\pi_{\mu_2 \mu_1} + \eta \sigma_{\mu_2 \mu_1}] + \frac{\xi_{3p}}{\eta} \frac{P^{\mu_2}}{T^3} [\Delta_{\mu_2 \lambda_2} \partial_{\lambda_1} \pi^{\lambda_1 \lambda_2}] \\ & + \frac{\xi_{4p}}{T^2 \eta^2} \pi^2, \end{aligned} \quad (2.30)$$

where the four scalar functions $\xi_{1p}, \xi_{2p}, \xi_{3p}, \xi_{4p}$ are linearly related to $\chi_{0p}, \chi_{1p}, \chi_{2p}$

$$\xi_{1p} = \chi_{1p} \frac{4\bar{p}^2}{(d+3)} - \frac{\chi_{2p} \bar{E}_p}{\eta\tau_\pi} (\eta\tau_\pi + \lambda_1), \quad (2.31a)$$

$$\xi_{2p} = \frac{\chi_{2p}}{T\tau_\pi} \bar{E}_p - \chi_{0p}, \quad (2.31b)$$

$$\xi_{3p} = -\chi_{2p} \frac{2\bar{p}^2}{(d+1)} + 2\chi_{0p} \frac{\eta}{s} \bar{E}_p + a_{P*} n'_p, \quad (2.31c)$$

$$\xi_{4p} = \chi_{1p} \frac{2\bar{p}^4}{(d-1)(d+1)} - \chi_{2p} \frac{\bar{E}_p \bar{p}^2}{(d-1)} - \chi_{0p} \frac{\eta}{s} \bar{E}_p^2 c_s^2 + a_{E*} n'_p \bar{E}_p, \quad (2.31d)$$

with $\bar{p} = p/T$ and $\bar{E}_p = E_p/T$.

The coefficients a_{E*} and a_{P*} come from Eq. (2.14) and are adjusted so that the Landau matching conditions are satisfied. More specifically, we choose δU_* and δT_* in Eq. (2.14) so

that

$$-\frac{P \cdot \delta U_*}{T} = a_{P*} \frac{P^{\mu_1}}{\eta T^3} [\Delta_{\mu_1 \lambda_2} \partial_{\lambda_1} \pi^{\lambda_1 \lambda_2}] , \quad (2.32a)$$

$$-E_p \frac{\delta T_*}{T^2} = a_{E*} \bar{E}_p \frac{\pi^2}{T^2 \eta^2} . \quad (2.32b)$$

Then integrating over $f_{\mathbf{p}}(X)$ to determine the stress tensor and demanding that Eq. (2.24) (which is a restatement of the Landau matching condition), we conclude that

$$a_{P*} = \frac{T \eta \tau_\pi}{s} - (1 + d) \left(\frac{\eta}{s} \right)^2 , \quad (2.33a)$$

$$a_{E*} = \frac{T \eta \tau_\pi}{4s} - \frac{d+3}{d-1} \frac{T \lambda_1}{4s} + \frac{d+1}{2(d-1)} \left(\frac{\eta}{s} \right)^2 . \quad (2.33b)$$

Despite being somewhat complicated, the functional form of $\delta f_{(2)}$ is severely constrained, and is bounded by the transport coefficients η , λ_1 and $\eta \tau_\pi$ through Eqs. (2.23), (2.28), and (2.29). For a single component classical gas with the quadratic ansatz $\alpha = 0$, Eq. (2.23) shows that $\mathcal{C}_p = \frac{\eta}{s}$, and the three scalar functions which determine $\delta f_{(2)}$ can be simplified to

$$\chi_{0p} = \frac{\eta}{2s} n_p , \quad \chi_{1p} = \frac{1}{4} \left(\frac{\eta}{s} \right)^2 n_p , \quad \chi_{2p} = \frac{1}{2} \left(\frac{\eta}{s} \right)^2 n_p . \quad (2.34)$$

We will discuss the implementation of $\delta f_{(2)}$ in the next section.

III. IMPLEMENTATION IN SIMULATIONS OF HEAVY ION COLLISIONS

In this section we will implement the $\delta f_{(2)}$ corrections in a 2+1 boost invariant hydrodynamic code. A full event-by-event simulation of heavy ion collisions with $\delta f_{(2)}$, together with a comparison to data, goes beyond the scope of this initial study. Nevertheless, the effect of $\delta f_{(2)}$ in larger simulations can be anticipated by understanding how the linear response is modified by $\delta f_{(2)}$. Indeed, the qualitative features of event-by-event hydrodynamic simulations of heavy ion collisions (including the correlations between the harmonics of different order) are reproduced by linear *and* quadratic response [8–10]. In central collisions the linear response is sufficient, and was recently used to produce one of the best estimates of the shear viscosity and its uncertainty to date [2]. We will calculate the linear response to a given deformation ϵ_n in order to estimate the influence of $\delta f_{(2)}$ on v_n .

In a given heavy ion event, the particle spectrum is expanded in harmonics

$$\frac{1}{p_T} \frac{dN}{dp_T d\phi_{\mathbf{p}}} = \frac{1}{2\pi p_T} \frac{dN}{dp_T} \left(1 + \sum_n v_n(p_T) e^{in(\phi_{\mathbf{p}} - \Psi_n(p_T))} + \text{complex conj.} \right) , \quad (3.1)$$

where $\phi_{\mathbf{p}}$ is the azimuthal angle around the beam pipe, and $v_n(p_T)$ are positive by definition. In a linear response approximation the n -th harmonic, $v_n(p_T)$, in the event is assumed to be proportional to the n -th cumulant, ϵ_n , which characterizes the deformation of the entropy distribution¹. Specifically, we first define the normalized entropy distribution at an time

¹ Note that we will use cumulants rather than moments to characterize the deformation [10, 13].

initial time τ_0

$$\rho(\mathbf{x}_\perp) \equiv \frac{\tau_0 s(\mathbf{x}_\perp)}{\int d^2x \tau_0 s(\mathbf{x}_\perp)}. \quad (3.2)$$

Writing the coordinates in the transverse plane $\mathbf{x}_\perp = (x, y)$ as a complex number, $z = x + iy = re^{i\phi}$, we define the first six cumulants characterizing the harmonic deformations of the initial distribution

$$\epsilon_1 e^{i\Phi_1} \equiv -\frac{\langle z^* z^2 \rangle}{\langle r^3 \rangle}, \quad (3.3a)$$

$$\epsilon_2 e^{i2\Phi_2} \equiv -\frac{\langle z^2 \rangle}{\langle r^2 \rangle}, \quad (3.3b)$$

$$\epsilon_3 e^{i3\Phi_3} \equiv -\frac{\langle z^3 \rangle}{\langle r^3 \rangle}, \quad (3.3c)$$

$$\epsilon_4 e^{i4\Phi_4} \equiv \frac{1}{\langle r^4 \rangle} \left[\langle z^4 \rangle - 3 \langle z^2 \rangle^2 \right], \quad (3.3d)$$

$$\epsilon_5 e^{i5\Phi_5} \equiv \frac{1}{\langle r^5 \rangle} \left[\langle z^5 \rangle - 10 \langle z^2 \rangle \langle z^3 \rangle \right], \quad (3.3e)$$

$$\epsilon_6 e^{i6\Phi_6} \equiv \frac{1}{\langle r^6 \rangle} \left[\langle z^6 \rangle - 15 \langle z^4 \rangle \langle z^2 \rangle - 10 \langle z^3 \rangle^2 + 30 \langle z^2 \rangle^3 \right], \quad (3.3f)$$

where $\langle \dots \rangle$ denote an average over $\rho(\mathbf{x}_\perp)$.

In a linear response approximation the orientation angle of n -th harmonic $\Psi_n(p_T)$ is aligned or anti-aligned with the cumulant angle Φ_n . Specifically, the spectrum in linear response is [13]

$$\frac{1}{p_T} \frac{dN}{dp_T d\phi_p} = \frac{1}{2\pi p_T} \frac{dN}{dp_T} \left(1 + 2 \sum_n w_n(p_T) \cos(n(\phi_p - \Phi_n)) + \dots \right). \quad (3.4)$$

Comparison with Eq. (3.1) shows that within this approximation scheme

$$v_n(p_T) = \sqrt{w_n^2(p_T)}, \quad (3.5)$$

and thus $w_n(p_T)$ differs at most by a sign from $v_n(p_T)$, *i.e.* $w_n(p_T) = v_n(p_T) \cos(n(\Psi_n(p_T) - \Phi_n))$. We will present the linear response coefficient, $w_n(p_T)/\epsilon_n$.

The linear response coefficient $w_n(p_T)/\epsilon_n$ is independent of many of the details of the initial state [13], and can be reasonably computed by initializing 2 + 1 boost invariant hydrodynamics with a deformed Gaussian distribution, where the rms radius and amplitude of the Gaussian are adjusted to match the rms radius and total entropy of the event. For example, to simulate w_3 at RHIC at an impact parameter of $b = 7.45$ fm we initialize a Gaussian deformed by $\epsilon_3 = 0.05$ with $\Phi_3 = 0$

$$\tau_0 s(\mathbf{x}, \tau_0) = C_s \langle N_p \rangle \left[1 + \frac{\langle r^3 \rangle \epsilon_3}{24} \left(\left(\frac{\partial}{\partial x} \right)^3 - 3 \left(\frac{\partial}{\partial y} \right)^2 \frac{\partial}{\partial x} \right) \right] \frac{e^{-\frac{r^2}{\langle r^2 \rangle}}}{\pi \langle r^2 \rangle}, \quad (3.6)$$

where C_s sets the total multiplicity in the event. Here $\langle r^2 \rangle$ and $\langle N_p \rangle$ are computed using the Phobos Glauber model [14]. In order that the total entropy closely matches the total

Momentum Dependence	$\eta\tau_\pi$	λ_1
Linear Ansatz ($\alpha = 1$)	$(d + 1) = 5$	$(d + 1)^2/(d + 3) = 25/7$
Quadratic Ansatz ($\alpha = 0$)	$(d + 2) = 6$	$(d + 2) = 6$

TABLE I. A compilation of rescaled second order transport coefficients for a linear and quadratic ansatz in a relaxation time approximation for classical statistics [4]. All numbers in this table should be *multiplied* by $\eta^2/(e + \mathcal{P})$. In a relaxation time approximation $\lambda_2 = -2\eta\tau_\pi$ and $\lambda_3 = 0$ [4].

entropy in more complete simulations [5, 15], we take $C_s = 15.9$ and 28.04 at RHIC and LHC respectively. This procedure has been used previously by the authors to determine the linear and non-linear response [10, 11, 13].

After initializing the Gaussian, we evolve the system with second order hydrodynamics, Eq. (2.4) and Eq. (2.8), using a variant of the central scheme developed previously [16, 17]. Then for a given n -th order harmonic perturbation ϵ_n we compute w_n/ϵ_n by performing the freezeout integral at a constant temperature. This evolution requires an equation of state and specified hydrodynamic parameters at first and second order. In what follows we will consider a conformal equation of state for a single component classical gas, and a lattice motivated equation of state previously used by Romatschke and Luzum [5].

Since it is only for the conformal equation of state $p = \frac{1}{3}\epsilon$ that the analysis of Section II is strictly valid we will discuss this case first, and then discuss the necessary modifications for a lattice based equation of state. To keep the final freezeout volume of the conformal equation of state approximately equal to the much more realistic lattice based equation of state, we choose the final freezeout temperature ($T_{\text{fo}} = 96$ MeV) so that the entropy density at freezeout $s_{\text{frz}} = 1.87 \text{ fm}^{-3}$ equals the entropy density of a hadron resonance gas at a temperature of $T = 150$ MeV. The relation between the temperature and energy density for the conformal equation of state is $e/T^4 = 12.2$, which is the value for a two flavor ideal quark-gluon plasma. The motivation for these choices, the parameters of the conformal equation of state, and further details about the initial conditions and freezeout we refer to our previous work – see especially Appendix B of Ref. [13].

The second order transport coefficients $\eta\tau_\pi$ and λ_1 are all constrained by the momentum dependence of the relaxation time and the shear viscosity through Eqs. (2.23), (2.28), (2.29). As discussed in Ref. [7], there are two limits for this momentum dependence which span the gamut of reasonable possibilities. In the first limit the relaxation time grows linearly with momentum, and $\alpha = 0$ in Eq. (2.12). This is known as the *quadratic ansatz*, and is most often used to simulate heavy ion collisions. In a similarly extreme limit the relaxation time is independent of momentum, and $\alpha = 1$ in Eq. (2.12). This is known as the *linear ansatz*, and this limit provides a useful foil to the more commonly adopted quadratic ansatz. Once the shear viscosity and the momentum dependence of the relaxation time are given, the collision kernel is completely specified in the relaxation time approximation, and all transport coefficients are fixed. For a linear and quadratic ansatz we record the appropriate second order transport coefficients in Table I.

So far this section has detailed the initial and freezeout conditions, as well as the second

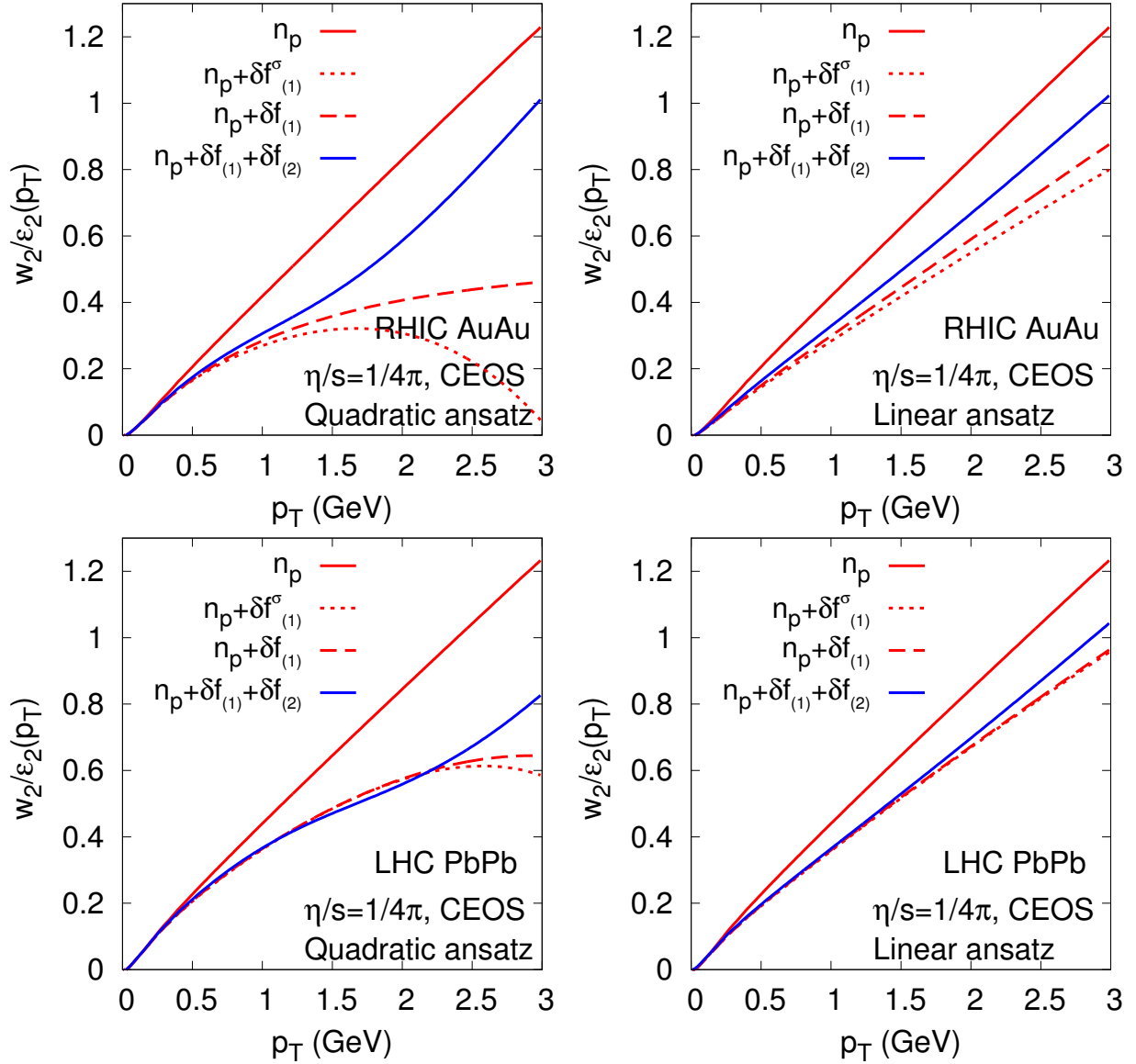


FIG. 1. Differential $w_2(p_T)/\epsilon_2$ for RHIC and LHC initial conditions, for a linear and quadratic ansatz, and a conformal equation of state (CEOS). The n_p curves show the flow from second order hydrodynamics without the viscous correction to the distribution function; $\delta f_{(1)}$ and $\delta f_{(1)} + \delta f_{(2)}$ show the flow with the viscous correction at first and second order; and finally, the $\delta f_{(1)}^\sigma$ result uses $-\eta\sigma^{\mu\nu}$ instead of $\pi^{\mu\nu}$ in the first order result (see Eq. (2.17)). The freezeout temperature is chosen so that the freezeout entropy density of the conformal gas equals that of a hadronic resonance gas at a temperature of $T = 150$ MeV.

order parameters which are used in the conformal equation of state. Fig. 1 shows the resulting elliptic flow for the quadratic and linear ansätze for a conformal equation of state including the first and second order δf . A conformal equation of state has a strong expansion, and, as a result, generally over estimates the magnitude of the δf correction. Thus the conformal analysis provides a schematic upper bound on the magnitude of the $\delta f_{(2)}$ correction. Further discussion of these results is reserved for Section IV

Strictly speaking the analysis of Section II is useful only for a single component conformal gas. Nevertheless, we believe the usefulness of the analysis extends beyond this limited regime [4]. Indeed, examining the steps in the derivation one finds that only very-few non conformal terms appear at each order. For instance, if non-conformal corrections are kept in Eq. (2.17) one finds

$$\delta f_{(1)\text{-non-conf}}^\sigma(\mathbf{p}) = \mathcal{C}_p n'_p \left[\frac{P^\mu P^\nu \sigma_{\mu\nu}}{2T^3} + \left(-\frac{E_{\mathbf{p}}^2 - p^2}{3T^3} + \frac{(\frac{1}{3} - c_s^2)E_{\mathbf{p}}^2}{T^3} \right) \nabla_\mu U^\mu \right], \quad (3.7)$$

which shows that non-conformal terms (the second term in Eq. (3.7)) are either suppressed by $\frac{1}{3} - c_s^2$, or are suppressed at high momentum relative to the conformal terms.

To extend our analysis to a multi-component non-conformal equation of state we have followed the simplified treatment that is used in almost all simulations of heavy ion collisions. First, we will treat all species independently

$$P^\mu \partial_\mu f_{\mathbf{p}}^a(X) = -\frac{T^2}{\mathcal{C}_p^a} [f_{\mathbf{p}}^a(X) - n^a(-P \cdot U_*(X)/T_*(X))] , \quad (3.8)$$

where $a = \pi, K, \rho, \dots$ is a species label². We will also adopt the quadratic ansatz $\alpha = 0$, so that \mathcal{C}_p^a is independent of momentum. Then for every species we define the partial entropy and shear viscosity as in Eqs. 2.23 and 2.25

$$\eta_a = \frac{-\mathcal{C}_p^a}{(d-1)(d+1)} \left[\frac{g_a}{T^3} \int_{\mathbf{p}} n_p^{a'} \frac{p^4}{E_p} \right], \quad (3.9a)$$

$$s_a = \frac{-1}{(d-1)} \left[\frac{g_a}{T^2} \int_{\mathbf{p}} n_p^{a'} p^2 \right], \quad (3.9b)$$

where g_a is the spin-isospin degeneracy factor. The full shear viscosity and entropy density is a sum of the partial results, $\eta = \sum_a \eta_a$ and $s = \sum_a s_a$. We require that η_a/s_a is equal to η/s for each species, and thus the relaxation time parameter \mathcal{C}_p^a is, in principle, different for each species. However, for a classical gas the two integrals in square brackets are equal upon integrating by parts, and thus $\mathcal{C}_p^a = \eta_a/s_a = \eta/s$ is independent of the mass and species label. For fermi-dirac and bose statistics these integrals are very nearly equal (to 4% accuracy) for all values of the mass, and \mathcal{C}_p^a is approximately equal to η/s for all species independent of mass and statistics.

Now that the relaxation time parameter \mathcal{C}_p^a is fixed for each species, the corresponding second order δf for each species is found by appending a species label, $n_p \rightarrow n_p^a$ and $\mathcal{C}_p \rightarrow \mathcal{C}_p^a$, to previous results. For a multi-component gas with a quadratic ansatz we find

$$\eta\tau_\pi + \lambda_1 = \sum_a (\mathcal{C}_p^a)^2 \left[\frac{2g_a}{(d-1)(d+1)(d+3)T^6} \int_{\mathbf{p}} n_p^{a''} \frac{p^6}{E_p} \right], \quad (3.10a)$$

$$\eta\tau_\pi = \sum_a (\mathcal{C}_p^a)^2 \left[\frac{-g_a}{(d-1)(d+1)T^5} \int_{\mathbf{p}} n_p^{a'} p^4 \right]. \quad (3.10b)$$

² There have been several efforts to go beyond this extreme species independent approximation [7, 18].

For classical statistics $\mathcal{C}_p^a = \eta/s$, and integrating the first integral in square brackets by parts yields a simple relation noted previously [4]

$$\lambda_1 = \eta\tau_\pi \quad (\text{for } \alpha = 0). \quad (3.11)$$

The remaining thermodynamic integrals are most easily done numerically; summing over all hadronic species with mass less than 1.5 GeV we find

$$\lambda_1 = \eta\tau_\pi = \frac{\eta^2}{(e + \mathcal{P})} 8.9. \quad (3.12)$$

Thus, $T\tau_\pi/(\eta/s) = 8.9$ would seem to be the most consistent value for the 2nd order transport coefficients during the hydrodynamic evolution of the hadronic phase. However, this value for $T\tau_\pi$ is somewhat too large to be used comfortably in the simulation [19]. Further, $T\tau_\pi$ decreases as temperature increases, and $T\tau_\pi/(\eta/s) \simeq 5$ is good approximation in the QGP phase [4]. We have therefore taken $\lambda_1 = \eta\tau_\pi = 5\eta^2/(e + \mathcal{P})$ throughout the evolution. This means that there is a small inconsistency between the second order δf at freezeout, and the second order parameters used to simulate the bulk of the hydrodynamic evolution. Similar inconsistencies are found in all attempts to consistently couple hydrodynamic codes with hadronic cascades [20].

To summarize, in this section we have specified precisely the initial conditions, the equation of state, the transport coefficients at first and second order, and the first and second order corrections to the distribution functions. We have used this setup to compute the linear response coefficients w_n/ϵ_n for RHIC and LHC initial conditions for the first six harmonics. Our results are displayed in Fig. 2 and Fig. 3. We will discuss the physics of these curves in the next section.

IV. DISCUSSION

This work computed the second order viscous correction to the thermal distribution function, $\delta f_{(2)}$, and used this result to estimate the effect of second order corrections on the harmonic spectrum. Our principle results are shown in Fig. 1 for a conformal equation of state, and Fig. 2, and Fig. 3 for a lattice based equation of state. First, examine the v_2 curves for the conformal EOS shown in Fig. 1. The most important remark is that even for a conformal equation of state, where the expansion is most violent, the derivative expansion converges acceptably for $p_T \lesssim 1.5$ GeV, *i.e.* the second order correction is small compared to the first order correction. Not surprisingly, when a linear ansatz is used for δf (rather than the more popular quadratic ansatz) the convergence of the derivative expansion is improved at high p_T . Typically in hydrodynamic simulations of heavy ion collisions, the strictly first order $\delta f_{(1)}^\sigma$ is replaced by the $\delta f_{(1)}$ which incorporates some, but not all, second order terms³. Examining Fig. 1, and also Fig. 2 and Fig. 3, we see that, while the sign of the second order correction is correctly reproduced by this incomplete treatment, the magnitude of the correction is generally significantly underestimated, and the p_T dependence of the second order correction is qualitatively wrong.

³ As discussed above, $\delta f_{(1)}$ uses $\pi^{\mu\nu}$ in place of $-\eta\sigma^{\mu\nu}$ when calculating the first order correction.

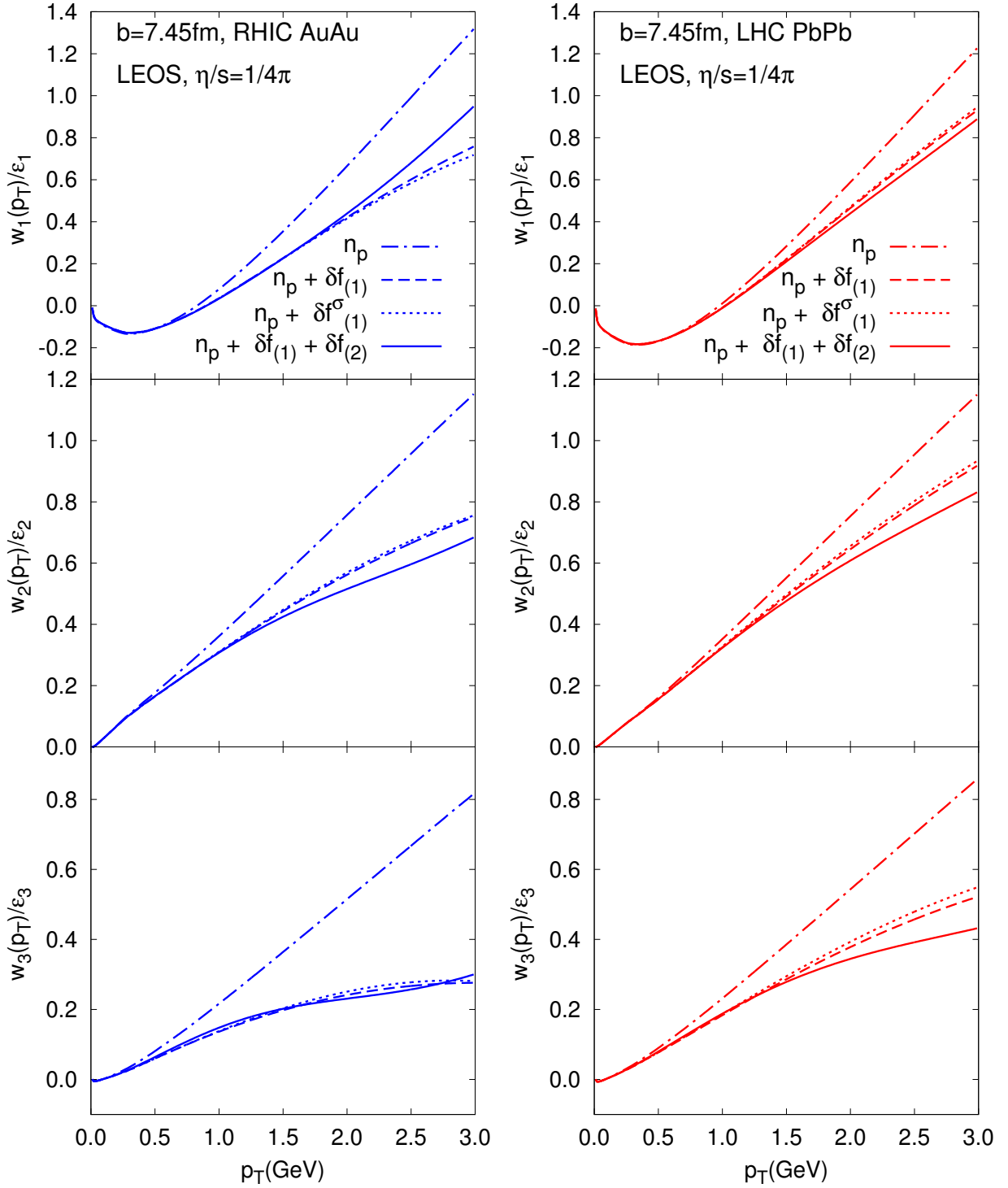


FIG. 2. Differential w_n/ϵ_n from various viscous hydrodynamic simulations at $b = 7.45$ fm for RHIC and LHC initial conditions, and a lattice equation of state (LEOS) with $T_0 = 150$ MeV. Here the n_p curve shows the flow from second order hydrodynamics without the viscous correction to the distribution function; $\delta f_{(1)}$ and $\delta f_{(1)} + \delta f_{(2)}$ show the flow with the viscous correction at first and second order respectively; and finally, the $\delta f_{(1)}^\sigma$ curve uses $-\eta\sigma^{\mu\nu}$ instead of $\pi^{\mu\nu}$ in the first order viscous correction (see Eq. (2.17)).

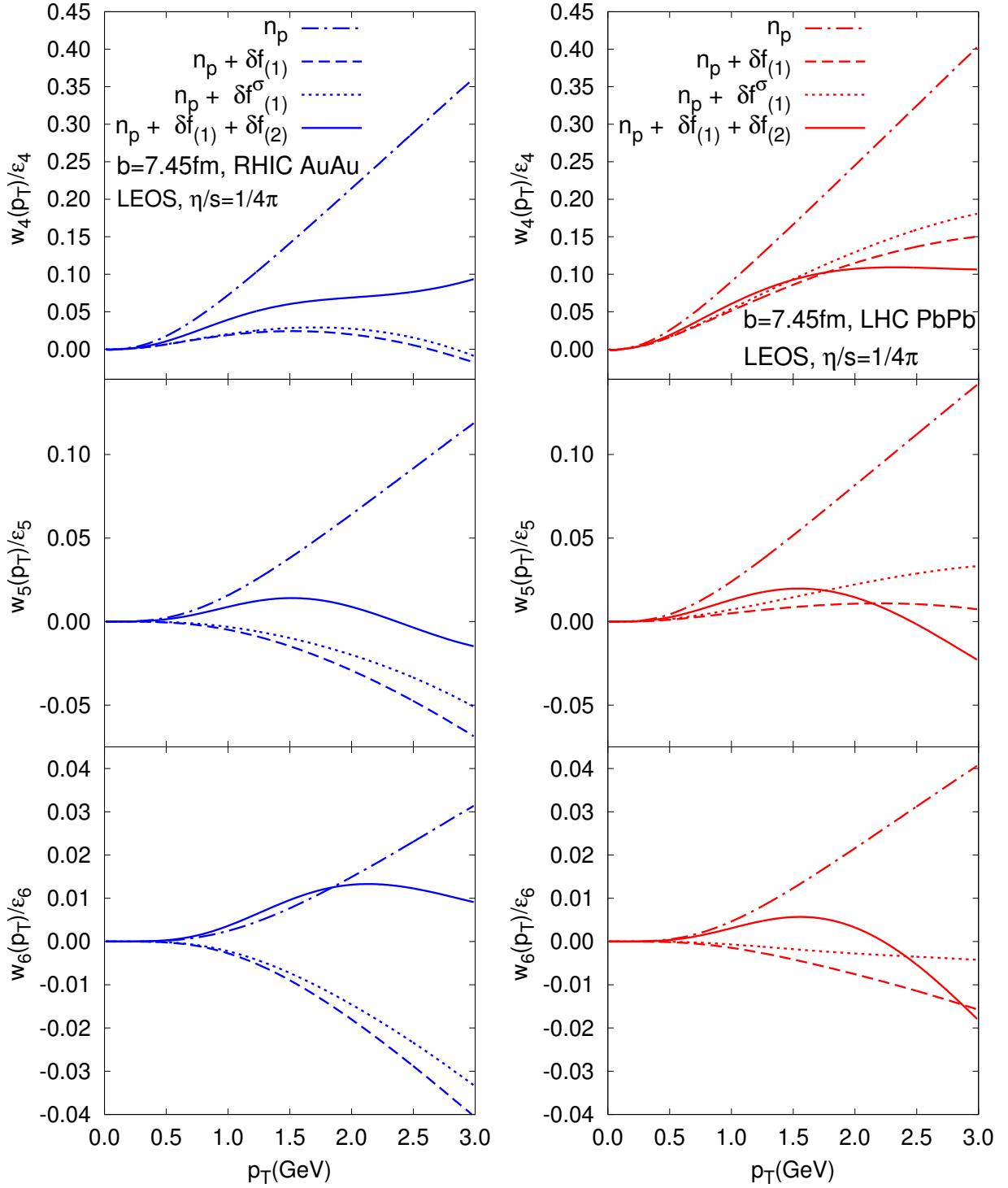


FIG. 3. Differential w_n/ϵ_n from various viscous hydrodynamic simulations at $b = 7.45$ fm for RHIC and LHC initial conditions, and a lattice equation of state (LEOS) with $T_{fo} = 150$ MeV. Here the n_p curve shows the flow from second order hydrodynamics without the viscous correction to the distribution function; $\delta f_{(1)}$ and $\delta f_{(1)} + \delta f_{(2)}$ show the flow with the viscous correction at first and second order respectively; and finally, the $\delta f_{(1)}^\sigma$ curve uses $-\eta\sigma^{\mu\nu}$ instead of $\pi^{\mu\nu}$ in the first order viscous correction (see Eq. (2.17)).

Most of these observations remain true for the more realistic lattice equation of state shown in Fig. 2 and Fig. 3. Generally, second order corrections are quite small for the first three harmonics, v_1 to v_3 , and become increasingly important as the harmonic number increases. Indeed, for v_6 at RHIC and the LHC, the second order viscous correction is of order one, and the hydrodynamic estimate can no longer be trusted. It is also instructive to note that the sign of the second order viscous correction for $p_T \lesssim 1.5 \text{ GeV}$ is positive, *i.e.* second order corrections bring the $v_n(p_T)$ curves closer to the ideal results. Generally, when the first order correction, becomes so large as to make w_n negative⁴, the second order correction conspires to keep w_n positive. When constraining η/s with hydrodynamic simulations, the second order corrections are most important for v_4 and v_5 . Indeed, at RHIC these corrections are quite important for v_5 even in central collisions.

For a practical perspective, using $\delta f_{(2)}$ in a hydrodynamic simulation is not particularly more difficult than using $\delta f_{(1)}$, and Eq. 2.18 can be readily implemented in most hydro codes. The functional form of $\delta f_{(2)}$ and its magnitude is about as well constrained as $\delta f_{(1)}$, and consistency with the second order hydrodynamic evolution would seem to mandate its use. At very least $\delta f_{(2)}$ should be taken into consideration when estimating the uncertainty in the η/s extracted from heavy ion collisions. Finally, when trying to use hydrodynamics in very small systems such as proton-nucleus collisions at RHIC and the LHC [21–27], second order corrections to δf should be used in order to monitor the convergence of the gradient expansion.

Acknowledgments:

We thank Ulrich Heinz for emphasizing that v_n is positive by definition. D. Teaney is a RIKEN-RBRC fellow. This work was supported in part by the Sloan Foundation and by the Department of Energy, DE-FG-02-08ER4154.

Appendix A: Tensor decomposition of $\delta f_{(2)}$

The goal of this appendix is to compute $\delta f_{(2)}$ and to record how this results transforms under rotations in the local rest frame. Our starting point is Eqs. (2.18) which we rewrite in terms of irreducible tensors under rotations in the local rest frame.

A systematic strategy decomposes all derivatives into temporal and spatial components

$$\partial_\mu = -U_\mu D + \nabla_\mu, \quad (\text{A1})$$

where the spatial component ∇_μ is orthogonal to U_μ . When differentiating a quantity that is already first order (*i.e.* $P^\mu \partial_\mu \delta f_{(1)}^\sigma$), we can use the lowest order conformal equations of motion to rewrite time derivatives in terms of spatial derivatives

$$D \ln T = -c_s^2 \nabla \cdot U, \quad (\text{A2})$$

$$DU_\mu = -\nabla_\mu \ln T, \quad (\text{A3})$$

⁴ v_n is positive by definition, see Eq. (3.1). Negative values of w_n indicate that the flow angle $\Psi_n(p_T)$ is anti-aligned with the participant angle plane, Φ_n .

where $c_s^2 = (e + \mathcal{P})/(Tc_v) = 1/(d-1)$. Finally, the resulting tensors can be decomposed into symmetric, traceless, and spatial tensors as in Eq. (2.2), which transform irreducibly under rotations in the local rest frame. To illustrate the procedure, we record the decomposition of $D\sigma_{\alpha\beta}$

$$D\sigma_{\alpha\beta} = D(\sigma^{\mu\nu}\Delta_{\mu\alpha}\Delta_{\nu\beta}) = \Delta_{\mu\alpha}\Delta_{\nu\beta}D\sigma^{\mu\nu} + \sigma^{\mu\nu}D(\Delta_{\mu\alpha}\Delta_{\nu\beta}), \quad (\text{A4})$$

$$= \langle D\sigma_{\alpha\beta} \rangle - (\sigma_{\beta}^{\mu}u_{\alpha}\nabla_{\mu}\ln T + u_{\beta}\sigma_{\alpha}^{\nu}\nabla_{\nu}\ln T). \quad (\text{A5})$$

Similarly, the symmetrized spatial tensor $\{\nabla_{\mu}\sigma_{\alpha\beta}\}_{\text{sym}}$ that arises when differentiating $\delta f_{(1)}^{\sigma}$ is decomposed as

$$\begin{aligned} \{\nabla_{\mu}\sigma_{\alpha\beta}\}_{\text{sym}} = & \langle \nabla_{\mu}\sigma_{\alpha\beta} \rangle + \left\{ \frac{2}{d+1}\Delta_{\mu\alpha}\nabla_{\gamma}\sigma_{\beta}^{\gamma} + u_{\alpha}\langle \sigma_{\beta}^{\rho}\sigma_{\mu\rho} \rangle \right. \\ & \left. + u_{\alpha}\frac{\Delta_{\mu\beta}}{d-1}\sigma^2 + 2u_{\alpha}\langle \sigma_{\beta}^{\rho}\Omega_{\mu\rho} \rangle + 2u_{\alpha}\frac{\sigma_{\mu\beta}}{d-1}\nabla \cdot U \right\}_{\text{sym}}, \end{aligned} \quad (\text{A6})$$

where we have used

$$\nabla_{\mu}u_{\rho} = \frac{1}{2}\sigma_{\mu\rho} + \Omega_{\mu\rho} + \frac{\Delta_{\mu\rho}}{d-1}\nabla \cdot U. \quad (\text{A7})$$

Finally, we note that

$$\langle \partial_{\lambda}\pi_{\mu}^{\lambda} \rangle = \Delta_{\mu\lambda_2}\partial_{\lambda_1}\pi^{\lambda_1\lambda_2} = -\eta \left[(d-2)\langle \sigma_{\mu\lambda}\nabla^{\lambda}\ln T \rangle + \langle \nabla_{\lambda}\sigma_{\mu}^{\lambda} \rangle \right], \quad (\text{A8})$$

where we have used the first order expression, $\pi^{\mu\nu} = -\eta\sigma^{\mu\nu}$, the conformal temperature dependence of $\eta \propto T^{d-1}$, and the lowest order equations of motion.

With this automated set of steps, we start with Eq. (2.18) and place $\delta f_{(2)}^{\sigma}$ into its canonical form

$$\begin{aligned} \delta f_{(2)}^{\sigma} = & \chi_{1p} \frac{P^{\mu_1}P^{\mu_2}P^{\mu_3}P^{\mu_4}}{T^6} \langle \sigma_{\mu_1\mu_2}\sigma_{\mu_3\mu_4} \rangle + \chi_{2p} \frac{P^{\mu_1}P^{\mu_2}P^{\mu_3}}{T^5} [\langle \nabla_{\mu_1}\sigma_{\mu_2\mu_3} \rangle - 3\langle \sigma_{\mu_1\mu_2}\nabla_{\mu_3}\ln T \rangle] \\ & + \left(\chi_{1p}\frac{4\bar{p}^2}{d+3} - \chi_{2p}\bar{E}_p \right) \frac{P^{\mu_2}P^{\mu_1}}{T^4} \langle \sigma_{\mu_2}^{\lambda}\sigma_{\mu_1\lambda} \rangle \\ & + \chi_{2p}\bar{E}_p \frac{P^{\mu_2}P^{\mu_1}}{T^4} \left[\langle D\sigma_{\mu_2\mu_1} \rangle + \frac{\sigma_{\mu_2\mu_1}}{d-1}\nabla \cdot U - 2\langle \sigma_{\mu_2}^{\lambda}\Omega_{\mu_1\lambda} \rangle \right] \\ & + \xi_{3p} \frac{P^{\mu_2}}{T^3} \left[-\langle \nabla_{\lambda}\sigma_{\mu_2}^{\lambda} \rangle - (d-2)\langle \sigma_{\mu_2\lambda}\nabla^{\lambda}\ln T \rangle \right] + \frac{\xi_{4p}}{T^2}\sigma^2, \end{aligned} \quad (\text{A9})$$

where the functions χ_{0p} , χ_{1p} , χ_{2p} and ξ_{3p} and ξ_{4p} are recorded in the text, Eq. (2.31).

In this form it is easy to integrate over the the phase space to determine the viscous stress

$$\pi^{\mu\nu} = \pi_{(1)}^{\mu\nu} + \pi_{(2)}^{\mu\nu} = \int_p \frac{P^{\mu}P^{\nu}}{P^0} (\delta f_{(1)}^{\sigma} + \delta f_{(2)}^{\sigma}), \quad (\text{A10})$$

where $\pi_{(1)}^{\mu\nu}$ and $\pi_{(2)}^{\mu\nu}$ are given by static form of the constituent relation Eq. (2.5). Rotational invariance in the rest frame reduces these tensor integrals, *e.g.*

$$\int_p \chi_{0p} \frac{P^{\mu_1}P^{\mu_2}P^{\mu_3}P^{\mu_4}}{P^0} \langle O_{\mu_3\mu_3} \rangle = \left[\frac{2}{(d-1)(d+1)} \int_p \chi_{0p} \frac{p^4}{E_p} \right] \langle O^{\mu_1\mu_2} \rangle, \quad (\text{A11})$$

yielding the equations for the transport coefficients written in the text, Eqs. (2.23), (2.28), and (2.29). In addition, we see that independent of the collision integral one finds the kinetic theory expectations identified in Ref. [4]

$$\lambda_2 = -2\eta\tau_\pi, \quad \text{and} \quad \lambda_3 = 0. \quad (\text{A12})$$

Finally, in presenting these results in the text, and in implementing the results in a realistic hydrodynamic simulation, we have used the dynamic form of second order hydrodynamics, where $\pi^{\mu\nu}$ is treated as a dynamic variable. This choice amounts to using $-\pi_{\mu\nu}/\eta$ in place of $\sigma_{\mu\nu}$. In $\delta f_{(2)}^\sigma$ this reparametrizations yields the replacements:

$$\langle D\sigma_{\mu_1\mu_2} \rangle + \frac{\sigma_{\mu_1\mu_2}}{d-1} \nabla \cdot U - 2 \langle \sigma_{\mu_1}^\lambda \Omega_{\mu_2\lambda} \rangle \rightarrow \frac{1}{\eta\tau_\pi} [\pi_{\mu_1\mu_2} + \eta\sigma_{\mu_1\mu_2}] - \frac{\lambda_1}{\eta\tau_\pi} \frac{1}{\eta^2} \langle \pi_{\mu_1}^\lambda \pi_{\mu_2\lambda} \rangle, \quad (\text{A13})$$

$$\langle \nabla_{\mu_1} \sigma_{\mu_2\mu_3} \rangle - 3 \langle \sigma_{\mu_1\mu_2} \nabla_{\mu_3} \ln T \rangle \rightarrow \frac{1}{\eta} [(d+2) \langle \pi_{\mu_1\mu_2} \nabla_{\mu_3} \ln T \rangle - \langle \nabla_{\mu_1} \pi_{\mu_2\mu_3} \rangle], \quad (\text{A14})$$

and Eq. (A8). In addition, when replacing $\sigma_{\mu\nu}$ with $-\pi_{\mu\nu}/\eta$ in the first order result, the difference $\frac{1}{\eta}(\pi_{\mu\nu} + \eta\sigma_{\mu\nu})$ must be appended to the second order result – see Eq. (2.19). The full result for $\delta f_{(1)}$ and $\delta f_{(2)}$ is given in Eqs. (2.20) and (2.30) respectively.

-
- [1] For an up to date review, see: Ulrich W Heinz and Raimond Snellings, “Collective flow and viscosity in relativistic heavy-ion collisions,” (2013), [arXiv:1301.2826 \[nucl-th\]](#).
 - [2] Matthew Luzum and Jean-Yves Ollitrault, “Extracting the shear viscosity of the quark-gluon plasma from flow in ultra-central heavy-ion collisions,” Nucl.Phys.A (2012), [arXiv:1210.6010 \[nucl-th\]](#).
 - [3] Rudolf Baier, Paul Romatschke, Dam Thanh Son, Andrei O. Starinets, and Mikhail A. Stephanov, “Relativistic viscous hydrodynamics, conformal invariance, and holography,” JHEP **0804**, 100 (2008), [arXiv:0712.2451 \[hep-th\]](#).
 - [4] Mark Abraao York and Guy D. Moore, “Second order hydrodynamic coefficients from kinetic theory,” Phys.Rev. **D79**, 054011 (2009), [arXiv:0811.0729 \[hep-ph\]](#).
 - [5] Matthew Luzum and Paul Romatschke, “Conformal Relativistic Viscous Hydrodynamics: Applications to RHIC results at $\sqrt{s} = 200$ GeV,” Phys. Rev. **C78**, 034915 (2008), [arXiv:0804.4015 \[nucl-th\]](#).
 - [6] See for example: Derek A. Teaney, “Viscous Hydrodynamics and the Quark Gluon Plasma,” (2009), invited review for ‘Quark Gluon Plasma 4’. Editors: R.C. Hwa and X.N. Wang, World Scientific, Singapore., [arXiv:0905.2433 \[nucl-th\]](#).
 - [7] Kevin Dusling, Guy D. Moore, and Derek Teaney, “Radiative energy loss and v(2) spectra for viscous hydrodynamics,” Phys.Rev. **C81**, 034907 (2010), [arXiv:0909.0754 \[nucl-th\]](#).
 - [8] Zhi Qiu and Ulrich W. Heinz, “Event-by-event shape and flow fluctuations of relativistic heavy-ion collision fireballs,” Phys.Rev. **C84**, 024911 (2011), [arXiv:1104.0650 \[nucl-th\]](#).

- [9] Fernando G. Gardim, Frederique Grassi, Matthew Luzum, and Jean-Yves Ollitrault, “Mapping the hydrodynamic response to the initial geometry in heavy-ion collisions,” *Phys.Rev.* **C85**, 024908 (2012), [arXiv:1111.6538 \[nucl-th\]](#).
- [10] Derek Teaney and Li Yan, “Non linearities in the harmonic spectrum of heavy ion collisions with ideal and viscous hydrodynamics,” *Phys.Rev.* **C86**, 044908 (2012), [arXiv:1206.1905 \[nucl-th\]](#).
- [11] Derek Teaney and Li Yan, “Non-linear flow response and reaction plane correlations,” (2012), [arXiv:1210.5026 \[nucl-th\]](#).
- [12] Derek Teaney, “Finite temperature spectral densities of momentum and R-charge correlators in N=4 Yang Mills theory,” *Phys.Rev.* **D74**, 045025 (2006), [arXiv:hep-ph/0602044 \[hep-ph\]](#).
- [13] Derek Teaney and Li Yan, “Triangularity and Dipole Asymmetry in Heavy Ion Collisions,” *Phys.Rev.* **C83**, 064904 (2011), [arXiv:1010.1876 \[nucl-th\]](#).
- [14] B. Alver, M. Baker, C. Loizides, and P. Steinberg, “The PHOBOS Glauber Monte Carlo,” (2008), [arXiv:0805.4411 \[nucl-ex\]](#).
- [15] Matthew Luzum, “Elliptic flow at energies available at the CERN Large Hadron Collider: Comparing heavy-ion data to viscous hydrodynamic predictions,” *Phys.Rev.* **C83**, 044911 (2011), [arXiv:1011.5173 \[nucl-th\]](#).
- [16] L. Pareschi, “Central differencing based numerical schemes for hyperbolic conservation laws with relaxation terms,” *SIAM Journal on Numerical Analysis* **39**, 1395–1417 (2001), <http://epubs.siam.org/doi/pdf/10.1137/S0036142900375906>.
- [17] K. Dusling and D. Teaney, “Simulating elliptic flow with viscous hydrodynamics,” *Phys.Rev.* **C77**, 034905 (2008), [arXiv:0710.5932 \[nucl-th\]](#).
- [18] G.S. Denicol and H. Niemi, “Derivation of transient relativistic fluid dynamics from the Boltzmann equation for a multi-component system,” (2012), [arXiv:1212.1473 \[nucl-th\]](#).
- [19] See for example: Huichao Song and Ulrich W. Heinz, “Causal viscous hydrodynamics in 2+1 dimensions for relativistic heavy-ion collisions,” *Phys.Rev.* **C77**, 064901 (2008), [arXiv:0712.3715 \[nucl-th\]](#).
- [20] Huichao Song, Steffen A. Bass, Ulrich Heinz, Tetsufumi Hirano, and Chun Shen, “Hadron spectra and elliptic flow for 200 A GeV Au+Au collisions from viscous hydrodynamics coupled to a Boltzmann cascade,” *Phys.Rev.* **C83**, 054910 (2011), [arXiv:1101.4638 \[nucl-th\]](#).
- [21] Serguei Chatrchyan *et al.* (CMS Collaboration), “Observation of long-range near-side angular correlations in proton-lead collisions at the LHC,” *Phys.Lett.* **B718**, 795–814 (2013), [arXiv:1210.5482 \[nucl-ex\]](#).
- [22] Betty Abelev *et al.* (ALICE Collaboration), “Long-range angular correlations on the near and away side in p-Pb collisions at $\sqrt{s_{NN}} = 5.02$ TeV,” *Phys.Lett.* **B719**, 29–41 (2013), [arXiv:1212.2001 \[nucl-ex\]](#).
- [23] Georges Aad *et al.* (ATLAS Collaboration), “Observation of Associated Near-side and Away-

- side Long-range Correlations in $\sqrt{s_{NN}} = 5.02$ TeV Proton-lead Collisions with the ATLAS Detector,” (2012), [arXiv:1212.5198 \[hep-ex\]](#).
- [24] Piotr Bozek and Wojciech Broniowski, “Correlations from hydrodynamic flow in p-Pb collisions,” *Phys.Lett. B* **718**, 1557–1561 (2013), [arXiv:1211.0845 \[nucl-th\]](#).
- [25] A. Adare *et al.* (PHENIX Collaboration), “Quadrupole anisotropy in dihadron azimuthal correlations in central d+Au collisions at $\sqrt{s_{NN}} = 200$ GeV,” (2013), [arXiv:1303.1794 \[nucl-ex\]](#).
- [26] Edward Shuryak and Ismail Zahed, “High Multiplicity pp and pA Collisions: Hydrodynamics at its Edge and Stringy Black Hole,” (2013), [arXiv:1301.4470 \[hep-ph\]](#).
- [27] Adam Bzdak, Bjoern Schenke, Prithwish Tribedy, and Raju Venugopalan, “Initial state geometry and the role of hydrodynamics in proton-proton, proton-nucleus and deuteron-nucleus collisions,” (2013), [arXiv:1304.3403 \[nucl-th\]](#).

Second order viscous corrections to the harmonic spectrum in heavy ion collisions

D. Teaney^{*} and L. Yan[†]

*Department of Physics & Astronomy,
Stony Brook University, Stony Brook, NY 11794, USA*

Abstract

We calculate the second order viscous correction to the kinetic distribution, $\delta f_{(2)}$, and use this result in a hydrodynamic simulation of heavy ion collisions to determine the complete second order correction to the harmonic spectrum, v_n . At leading order in a conformal fluid, the first viscous correction is determined by one scalar function, χ_{0p} . One moment of this scalar function is constrained by the shear viscosity. At second order in a conformal fluid, we find that $\delta f(\mathbf{p})$ can be characterized two scalar functions of momentum, χ_{1p} and χ_{2p} . The momentum dependence of these functions is largely determined by the kinematics of the streaming operator. Again, one moment of these functions is constrained by the parameters of second order hydrodynamics, τ_π and λ_1 . The effect of $\delta f_{(2)}$ on the integrated flow is small (up to v_4), but is quite important for the higher harmonics at modestly-large p_T . Generally, $\delta f_{(2)}$ increases the value of v_n at a given p_T , and is most important in small systems.

^{*} derek.teaney@stonybrook.edu

[†] li.yan@stonybrook.edu

I. INTRODUCTION

Motivated by the wealth of data on collective flow in heavy ion collisions, hydrodynamic simulations of these ultra-relativistic events have steadily improved. Today, event by event viscous hydrodynamic simulations reproduce the elliptic flow, the triangular flow, the higher harmonic flows, and the correlations between the flow harmonics and event plane angles [1]. The overall agreement with the data on this rich variety of observables constrains the shear viscosity of the QGP close to transition region. Because this success, there is a current need to precisely quantify the systematic uncertainties in these simulations and the corresponding uncertainty in the extracted shear viscosity of the QGP [2]. This paper will address this need by computing the second order corrections to the thermal distribution function [3, 4] and by using these results to simulate the observed harmonic spectrum.

Since the nucleus is not vastly larger than the mean free path, an important advance in hydrodynamic simulations was the inclusion of viscous corrections to the hydrodynamic equations of motion at first and second order in the gradient expansion. In particular Baier, Romatschke, Son, Starinets, Stephanov (BRSSS) determined the possible tensor forms that arise in the constituent relation of a conformal fluid at second order [3]. These equations are currently used in practically all viscous simulations of heavy ion collisions. It is satisfying that the gradient expansion, which underlies the hydrodynamic approach, seems to converge [5], and seems to converge to the measured flow [1]. However, all simulations of heavy ion collisions make additional kinetic assumptions about the fluid at freezeout when computing the particle spectra [6]. Indeed, the phase space distribution of a viscous fluid $f_{\mathbf{p}}(X)$ is modified from its equilibrium form, $n_{\mathbf{p}}(X)$, by corrections at first and second order, $\delta f_{\mathbf{p}} = \delta f_{(1)} + \delta f_{(2)}$. Currently, all simulations of heavy ion collisions compute the viscous corrections to the distribution function at first order, while using second order corrections to the hydrodynamic equations of motion. The goal of this work is to remedy this inconsistency by computing viscous corrections to the distribution function to second order. Then, this second order correction is used to compute the harmonic spectrum, $v_n(p_T)$. As expected [7], these corrections are modest for small harmonic numbers, n , and small p_T , but grow both with n and p_T .

To compute the viscous corrections to the phase space distribution we will analyze kinetic theory of a conformal gas close to equilibrium in a relaxation time approximation. This extreme idealization is still useful for several reasons. First, a similar equilibrium analysis of QCD kinetic theory was used to determine the second order transport coefficients to leading order in α_s [4]. This analysis (which will be discussed further below) makes clear that the details of the collision integral hardly matter in determining the second order transport coefficients. Indeed, we will see that the structure of the second order viscous correction $\delta f_{(2)}$ is largely determined by the kinematics of free streaming, rather than the details of the collision integral. Thus, an analysis based on a relaxation time approximation is an easy way to reliably estimate the size of such second order corrections in heavy ion collisions. Second, the overall normalization of $\delta f_{(2)}$ is constrained by the second order transport coefficients τ_π and λ_1 , in much the same way that the shear viscosity constrains the normalization of $\delta f_{(1)}$. These constraints allow us to make a good estimate of the form of viscous corrections at second order for a realistic non-conformal fluid.

With this functional form we study the effect of $\delta f_{(2)}$ on the harmonic spectrum in heavy ion collisions. In Section II we outline how $\delta f_{(2)}$ is computed in kinetic theory. Then, in

Section III we discuss the practical implementation of this formula in a hydrodynamic code used to simulate heavy ion collisions. These results are used to simulate the linear response to a given deformation, ϵ_n . The linear response is largely responsible for determining the v_n in central collisions. In non-central collisions the linear response *and* the quadratic response determine the harmonic flow and its correlations [1, 8–11], but the quadratic response will not be discussed in this initial study. Finally, we will summarize the effects of $\delta f_{(2)}$ in Section IV.

II. 2ND ORDER CORRECTIONS TO THE PHASE SPACE DISTRIBUTION

A. Notation

Throughout the paper we will work with the metric $\eta^{\mu\nu} = (-, +, +, +)$, and $d = 4$ denotes the number of space-time dimensions. Capital letters P, X denote four vectors, while lower case letters \mathbf{p}, \mathbf{x} denote three vectors in the rest frame.

We are expanding around a fluid in equilibrium with energy density, pressure, and flow velocity equal to $e(X)$, $\mathcal{P}(X)$, and $U^\mu(X)$ respectively where $U^\mu U_\mu = -1$. Thus, the rest frame projector is $\Delta^{\mu\nu} = g^{\mu\nu} + U^\mu U^\nu$, and the spatial derivatives and temporal derivatives are $\nabla^\mu = \Delta^{\mu\nu} \partial_\nu$ and $D = U^\mu \partial_\mu$, respectively. Finally bracketed tensors are rendered symmetric-traceless and orthogonal to U^μ ,

$$\langle A^{\mu\nu} \rangle = \frac{1}{2} \Delta^\mu_\rho \Delta^\nu_\sigma (A^{\rho\sigma} + A^{\sigma\rho}) - \frac{1}{(d-1)} \Delta^{\mu\nu} \Delta_{\rho\sigma} A^{\rho\sigma}. \quad (2.1)$$

Such tensors transform irreducibly under rotation in the local rest frame. A more elaborate example using $\sigma_{\mu\nu} = 2 \langle \nabla_\mu U_\nu \rangle$ which appears in the algebra below is

$$\begin{aligned} \{\sigma_{\mu_1\mu_2}\sigma_{\mu_3\mu_4}\}_{\text{sym}} &= \langle \sigma_{\mu_1\mu_2}\sigma_{\mu_3\mu_4} \rangle + \frac{4}{d+3} \{\Delta_{\mu_1\mu_2} \langle \sigma_{\mu_3}^\lambda \sigma_{\mu_4\lambda} \rangle\}_{\text{sym}} \\ &\quad + \frac{2}{(d-1)(d+1)} \{\Delta_{\mu_1\mu_2} \Delta_{\mu_3\mu_4}\}_{\text{sym}} \sigma^2, \end{aligned} \quad (2.2)$$

where the symmetrized spatial tensor is denoted with curly brackets:

$$\{\sigma_{\mu_1\mu_2}\sigma_{\mu_3\mu_4}\}_{\text{sym}} = \frac{1}{3} [\sigma_{\mu_1\mu_2}\sigma_{\mu_3\mu_4} + \sigma_{\mu_1\mu_3}\sigma_{\mu_2\mu_4} + \sigma_{\mu_1\mu_4}\sigma_{\mu_2\mu_3}]. \quad (2.3)$$

The equilibrium distribution function is $n_{\mathbf{p}} \equiv n(-P \cdot U(X)/T(X))$ where $n(z) = 1/(e^z \mp 1)$, and $f_{\mathbf{p}}(X)$ denotes the full non-equilibrium distribution. The rest frame integrals are abbreviated $\int_{\mathbf{p}} \equiv \int d^{d-1}p/(2\pi)^{d-1}$ and primes (such as $n'_{\mathbf{p}}$) denote derivatives with respect to $-P \cdot U/T$, so that $n'_{\mathbf{p}} = -n_{\mathbf{p}}(1 \pm n_{\mathbf{p}})$. The energy and squared three momentum in the rest frame are, $E_{\mathbf{p}} = -P \cdot U$ and $p^2 = P^\mu P^\nu \Delta_{\mu\nu}$, respectively.

B. Hydrodynamics

In evaluating $\delta f_{(2)}$ to second order we will need the hydrodynamic equations of motion. In the Landau frame these equations read

$$T^{\mu\nu} = eU^\mu U^\nu + \mathcal{P}\Delta^{\mu\nu} + \pi^{\mu\nu}, \quad \partial_\mu T^{\mu\nu} = 0, \quad (2.4)$$

where $\pi^{\mu\nu}$ is the viscous correction to the stress tensor. Throughout this analysis we are working with a conformal fluid, and consequently the bulk viscosity is zero $\zeta = 0$. For a conformal fluid the possible tensor forms of the gradient expansion for $\pi^{\mu\nu}$ through second order were established by BRSSS

$$\pi^{\mu\nu} = \pi_{(1)}^{\mu\nu} + \pi_{(2)}^{\mu\nu} + \dots = -\eta\sigma^{\mu\nu} + \eta\tau_\pi \left[\langle D\sigma^{\mu\nu} \rangle + \frac{1}{d-1}\sigma^{\mu\nu}\partial \cdot U \right] + \lambda_1 \langle \sigma^\mu{}_\lambda \sigma^{\nu\lambda} \rangle + \lambda_2 \langle \sigma^\mu{}_\lambda \Omega^{\nu\lambda} \rangle + \lambda_3 \langle \Omega^\mu{}_\lambda \Omega^{\nu\lambda} \rangle + \dots, \quad (2.5)$$

where $-\eta\sigma^{\mu\nu} = -2\eta \langle \nabla^\mu U^\nu \rangle$ is the first order term, and the vorticity tensor is

$$\Omega^{\mu\nu} = \frac{1}{2} \Delta^{\mu\alpha} \Delta^{\nu\beta} (\partial_\alpha U_\beta - \partial_\beta U_\alpha). \quad (2.6)$$

The ellipses in Eq. (2.5) denote terms third order in the gradients. Using these equations of motion, the time derivatives of the energy density and flow velocity can be determined from the spatial gradients of these fields

$$De = -(e + \mathcal{P})\nabla \cdot U + \frac{\eta}{2}\sigma_{\mu\nu}\sigma^{\mu\nu} + \dots, \quad (2.7a)$$

$$DU_\mu = -\frac{\Delta_\mu \mathcal{P}}{e + \mathcal{P}} - \frac{\Delta_{\mu\lambda_2} \partial_{\lambda_1} \pi^{\lambda_1\lambda_2}}{e + \mathcal{P}}, \quad (2.7b)$$

$$= -\frac{\nabla_\alpha \mathcal{P}}{e + \mathcal{P}} + \frac{\eta}{e + \mathcal{P}} [(d-2) \langle \sigma_{\mu\lambda} \nabla^\lambda \ln T \rangle + \langle \nabla_\lambda \sigma^\lambda{}_\mu \rangle] + \dots. \quad (2.7c)$$

In passing from Eq. (2.7b) to Eq. (2.7c) we have used the first order expression for $\pi^{\mu\nu} = -\eta\sigma^{\mu\nu}$, the conformal temperature dependence of $\eta \propto T^{d-1}$, and the lowest order equations of motion.

In hydrodynamic simulations of heavy ion collisions the static form of the constituent relation Eq. (2.5) is not used. Rather, this equation is rewritten as a dynamical equation for $\pi_{\mu\nu}$ which is evolved numerically [3]

$$\pi^{\mu\nu} = -\eta\sigma^{\mu\nu} - \tau_\pi \left[\langle D\pi^{\mu\nu} \rangle + \frac{d}{d-1}\pi^{\mu\nu}\nabla \cdot U \right] + \frac{\lambda_1}{\eta^2} \langle \pi^\mu{}_\lambda \pi^{\nu\lambda} \rangle - \frac{\lambda_2}{\eta} \langle \pi^\mu{}_\lambda \Omega^{\nu\lambda} \rangle + \lambda_3 \langle \Omega^\mu{}_\lambda \Omega^{\nu\lambda} \rangle. \quad (2.8)$$

Similarly, when constructing δf at first and second order we will systematically replace $\sigma_{\mu\nu}$ with $-\pi_{\mu\nu}/\eta$. For fluids with an underlying kinetic description, the transport coefficients are additionally constrained, with $\lambda_3 = 0$ and $\lambda_2 = -2\eta\tau_\pi$ [4], and these relations used in the simulation. The appropriate values for λ_1 and $\eta\tau_\pi$ will be discussed below.

C. Kinetics

To determine the viscous corrections to the distribution function we will solve the kinetic equations in a relaxation time approximation through second order in the gradient expansion

$$f_{\mathbf{p}} \equiv n_{\mathbf{p}} + \delta f_{\mathbf{p}} = n_{\mathbf{p}} + \delta f_{(1)} + \delta f_{(2)} + \dots. \quad (2.9)$$

In a relaxation time approximation the Boltzmann equation reads

$$P^\mu \partial_\mu f_{\mathbf{p}}(X) = -\frac{T^2}{\mathcal{C}_p} [f_{\mathbf{p}}(X) - n(-P \cdot U_*(X)/T_*(X))] , \quad (2.10)$$

where the dimensionless coefficient \mathcal{C}_p is related to the canonically defined momentum dependent relaxation time

$$\mathcal{C}_p = T^2 \frac{\tau_R(E_p)}{E_p} . \quad (2.11)$$

Following Ref. [7], we will parametrize the momentum dependence of the relaxation time as a simple power law

$$\tau_R \propto E_{\mathbf{p}}^{1-\alpha} , \quad (2.12)$$

with α between zero and one. As we will see below, $\alpha = 0$ gives a first order a viscous correction which grows quadratically with momentum (which is known as the quadratic ansatz), while $\alpha = 1$ gives a first order viscous correction which grows linearly with momentum (and is known as the linear ansatz).

At leading order, the parameters T_* and U_*^μ which appear in the kinetic equation are equal to the Landau matched temperature and flow velocity, T and U^μ . However, starting at second order T_* and U_*^μ will differ from T and U^μ by squares of gradients:

$$T_*(X) \equiv T(X) + \delta T_*(X) , \quad (2.13a)$$

$$U_*^\mu(X) \equiv U^\mu(X) + \delta U_*^\mu(X) . \quad (2.13b)$$

δT_* and δU_*^μ will be determined at each order by the Landau matching condition:

$$T^{\mu\nu} U_\nu = e U^\mu .$$

Expanding $n(-P \cdot U_*/T_*)$ we have

$$n_{\mathbf{p}}^* \equiv n_{\mathbf{p}} + \delta n_{\mathbf{p}}^* \quad \delta n_{\mathbf{p}}^* = n'_{\mathbf{p}} \left[-\frac{P \cdot \delta U_*}{T} - E_p \frac{\delta T_*}{T^2} \right] + \dots , \quad (2.14)$$

where we have used an obvious notation, $n_{\mathbf{p}}^* \equiv n(-P \cdot U_*/T_*)$ and $n_{\mathbf{p}} \equiv n(-P \cdot U/T)$.

Then to determine δf we substitute the expansion (Eq. (2.9)) into the relaxation time equation and equate orders. In doing so we use the hydrodynamic equations of motion through second order to write time derivatives of $T(X)$ and $U^\mu(X)$ in terms of spatial gradients of these fields. For instance, using the equations of motion Eq. (2.7) and the thermodynamic identities

$$c_v = \frac{de}{dT} , \quad \frac{1}{T(e + \mathcal{P})} d\mathcal{P} + d\left(\frac{1}{T}\right) = 0 , \quad c_s^2 = \frac{e + \mathcal{P}}{T c_v} , \quad (2.15)$$

and the relations $p^2 = E_p^2$ and $c_s^2 = 1/(d-1)$ of a conformal gas, we have

$$P^\mu \partial_\mu n_{\mathbf{p}} = -n'_{\mathbf{p}} \frac{p^\mu p^\nu}{2T} \sigma_{\mu\nu} - \frac{n'_{\mathbf{p}}}{(e+p)T} \left[-E_p P^{\mu_1} \Delta_{\mu_1 \mu_2} \partial_\lambda \pi^{\lambda \mu_2} + \frac{1}{2} E_p^2 c_s^2 \eta \sigma^2 \right] + \dots \quad (2.16)$$

The term linearly proportional to $\sigma_{\mu\nu}$ is ultimately responsible for the shear viscosity, while the nonlinear terms contribute to $\delta f_{(2)}$.

With this discussion, we find that the δf is determined by the hierarchy of equations:

$$\delta f_{(1)}^\sigma = \mathcal{C}_p n'_p \frac{P^\mu P^\nu \sigma_{\mu\nu}}{2T^3}, \quad (2.17)$$

and

$$\delta f_{(2)}^\sigma = \delta n_{\mathbf{p}}^* + \frac{\mathcal{C}_p n'_p}{(e+p)T^3} \left[-E_p P^{\mu_1} \Delta_{\mu_1 \mu_2} \partial_\lambda \pi^{\lambda \mu_2} + \frac{1}{2} E_p^2 c_s^2 \eta \sigma^2 \right] - \frac{\mathcal{C}_p}{T^2} P^\mu \partial_\mu \delta f_{(1)}^\sigma. \quad (2.18)$$

Straightforward algebra uses the equations of motion to decompose $\delta f_{(2)}$ into irreducible tensors, and determines the final form of $\delta f_{(1)}^\sigma$ and $\delta f_{(2)}^\sigma$ (see Appendix A).

We have put a superscript σ in $f_{(1)}^\sigma$ and $\delta f_{(2)}^\sigma$ to indicate that that we are using $\sigma_{\mu\nu}$ rather than $\pi_{\mu\nu}$ in these equations. In realistic hydrodynamic simulations of heavy ion collisions $\pi_{\mu\nu}$ is treated as a dynamic variable, and $-\eta\sigma_{\mu\nu}$ is systematically replaced by $\pi_{\mu\nu}$. This yields the following reparametrization of δf

$$\delta f_{(1)} = -\frac{1}{2} \mathcal{C}_p n'_p \frac{P^\mu P^\nu}{\eta T^3} \pi_{\mu\nu}, \quad (2.19a)$$

$$\delta f_{(2)} = \delta f_{(2)}^\sigma + \frac{1}{2} \mathcal{C}_p n'_p \frac{P^\mu P^\nu}{\eta T^3} [\pi_{\mu\nu} + \eta \sigma_{\mu\nu}], \quad (2.19b)$$

where we have replaced $\sigma_{\mu\nu}$ with $-\pi_{\mu\nu}/\eta$ in the first order result, and appended the difference between these two tensors to the second order result so that, $\delta f_{(1)} + \delta f_{(2)} = \delta f_{(1)}^\sigma + \delta f_{(2)}^\sigma$ up to third order terms.

To record the result for $\delta f_{(2)}$, we first review the familiar first order case. At first order, $\delta f_{(1)}$ is described by a dimensionless scalar function $\chi_{0p}(E_p/T)$

$$\delta f_1 = \chi_{0p} \frac{P^{\mu_1} P^{\mu_2}}{\eta T^3} \pi_{\mu_1 \mu_2}, \quad (2.20)$$

which has been extensively studied in the literature, and determines the shear viscosity [7]. In the relaxation time approximation this function is related to the relaxation time

$$\chi_{0p} = -\frac{1}{2} \mathcal{C}_p n'_p. \quad (2.21)$$

One moment of this function is constrained by the shear viscosity. Indeed, from the defining relation

$$\pi^{\mu\nu} = \int_{\mathbf{p}} \frac{P^\mu P^\nu}{P^0} \delta f_{\mathbf{p}}, \quad (2.22)$$

we determine the shear viscosity

$$\eta = \frac{2}{(d-1)(d+1)T^3} \int_{\mathbf{p}} \frac{p^4}{E_p} \chi_{0p}, \quad (2.23)$$

and a constraint on $\delta f_{(2)}$

$$0 = \int_{\mathbf{p}} \frac{P^\mu P^\nu}{P^0} \delta f_{(2)}. \quad (2.24)$$

This constraint reflects the reparametrization of $\sigma^{\mu\nu}$ in the first order $\delta f_{(1)}$ with $\pi^{\mu\nu}$. For later use and comparison, we note that the enthalpy is

$$(e + \mathcal{P}) = \frac{-1}{(d-1)T} \int_{\mathbf{p}} n'_p p^2, \quad (2.25)$$

which can be obtained by comparing the stress tensor from kinetic theory for small fluid velocities (*i.e.* $U^\mu \simeq (1, \mathbf{v})$ with $\mathbf{v} \ll 1$) to ideal hydrodynamics, $T^{0i} \simeq (e + \mathcal{P})v^i$ [12].

At second order the function $\delta f_{(2)}$ is described by two dimensionless scalar functions χ_{1p} and χ_{2p}

$$\chi_{1p} = -\frac{1}{2} \mathcal{C}_p \chi'_{0p}, \quad (2.26)$$

$$\chi_{2p} = \mathcal{C}_p \chi_{0p}. \quad (2.27)$$

Two moments of these scalar functions are constrained by the second order transport coefficients $\eta\tau_\pi$ and λ_1

$$\lambda_1 + \eta\tau_\pi = \frac{8}{(d-1)(d+1)(d+3)T^6} \int_{\mathbf{p}} \chi_{1p} \frac{p^6}{E_p}, \quad (2.28)$$

$$\eta\tau_\pi = \frac{2}{(d-1)(d+1)T^5} \int_{\mathbf{p}} \chi_{2p} p^4. \quad (2.29)$$

Then the functional form of $\delta f_{(2)}$ is

$$\begin{aligned} \delta f_{(2)} = & \frac{\chi_{1p}}{\eta^2} \frac{P^{\mu_1} P^{\mu_2} P^{\mu_3} P^{\mu_4}}{T^6} \langle \pi_{\mu_1 \mu_2} \pi_{\mu_3 \mu_4} \rangle + \frac{\chi_{2p}}{\eta} \frac{P^{\mu_1} P^{\mu_2} P^{\mu_3}}{T^5} [(d+2) \langle \pi_{\mu_1 \mu_2} \nabla_{\mu_3} \ln T \rangle - \langle \nabla_{\mu_1} \pi_{\mu_2 \mu_3} \rangle] \\ & + \frac{\xi_{1p}}{\eta^2} \frac{P^{\mu_2} P^{\mu_1}}{T^4} \langle \pi_{\mu_2}^\lambda \pi_{\mu_1 \lambda} \rangle + \frac{\xi_{2p}}{\eta} \frac{P^{\mu_2} P^{\mu_1}}{T^3} [\pi_{\mu_2 \mu_1} + \eta \sigma_{\mu_2 \mu_1}] + \frac{\xi_{3p}}{\eta} \frac{P^{\mu_2}}{T^3} [\Delta_{\mu_2 \lambda_2} \partial_{\lambda_1} \pi^{\lambda_1 \lambda_2}] \\ & + \frac{\xi_{4p}}{T^2 \eta^2} \pi^2, \end{aligned} \quad (2.30)$$

where the four scalar functions $\xi_{1p}, \xi_{2p}, \xi_{3p}, \xi_{4p}$ are linearly related to $\chi_{0p}, \chi_{1p}, \chi_{2p}$

$$\xi_{1p} = \chi_{1p} \frac{4\bar{p}^2}{(d+3)} - \frac{\chi_{2p} \bar{E}_p}{\eta\tau_\pi} (\eta\tau_\pi + \lambda_1), \quad (2.31a)$$

$$\xi_{2p} = \frac{\chi_{2p}}{T\tau_\pi} \bar{E}_p - \chi_{0p}, \quad (2.31b)$$

$$\xi_{3p} = -\chi_{2p} \frac{2\bar{p}^2}{(d+1)} + 2\chi_{0p} \frac{\eta}{s} \bar{E}_p + a_{P*} n'_p, \quad (2.31c)$$

$$\xi_{4p} = \chi_{1p} \frac{2\bar{p}^4}{(d-1)(d+1)} - \chi_{2p} \frac{\bar{E}_p \bar{p}^2}{(d-1)} - \chi_{0p} \frac{\eta}{s} \bar{E}_p^2 c_s^2 + a_{E*} n'_p \bar{E}_p, \quad (2.31d)$$

with $\bar{p} = p/T$ and $\bar{E}_p = E_p/T$.

The coefficients a_{E*} and a_{P*} come from Eq. (2.14) and are adjusted so that the Landau matching conditions are satisfied. More specifically, we choose δU_* and δT_* in Eq. (2.14) so

that

$$-\frac{P \cdot \delta U_*}{T} = a_{P*} \frac{P^{\mu_1}}{\eta T^3} [\Delta_{\mu_1 \lambda_2} \partial_{\lambda_1} \pi^{\lambda_1 \lambda_2}] , \quad (2.32a)$$

$$-E_p \frac{\delta T_*}{T^2} = a_{E*} \bar{E}_p \frac{\pi^2}{T^2 \eta^2} . \quad (2.32b)$$

Then integrating over $f_{\mathbf{p}}(X)$ to determine the stress tensor and demanding that Eq. (2.24) (which is a restatement of the Landau matching condition), we conclude that

$$a_{P*} = \frac{T \eta \tau_\pi}{s} - (1 + d) \left(\frac{\eta}{s} \right)^2 , \quad (2.33a)$$

$$a_{E*} = \frac{T \eta \tau_\pi}{4s} - \frac{d+3}{d-1} \frac{T \lambda_1}{4s} + \frac{d+1}{2(d-1)} \left(\frac{\eta}{s} \right)^2 . \quad (2.33b)$$

Despite being somewhat complicated, the functional form of $\delta f_{(2)}$ is severely constrained, and is bounded by the transport coefficients η , λ_1 and $\eta \tau_\pi$ through Eqs. (2.23), (2.28), and (2.29). For a single component classical gas with the quadratic ansatz $\alpha = 0$, Eq. (2.23) shows that $\mathcal{C}_p = \frac{\eta}{s}$, and the three scalar functions which determine $\delta f_{(2)}$ can be simplified to

$$\chi_{0p} = \frac{\eta}{2s} n_p , \quad \chi_{1p} = \frac{1}{4} \left(\frac{\eta}{s} \right)^2 n_p , \quad \chi_{2p} = \frac{1}{2} \left(\frac{\eta}{s} \right)^2 n_p . \quad (2.34)$$

We will discuss the implementation of $\delta f_{(2)}$ in the next section.

III. IMPLEMENTATION IN SIMULATIONS OF HEAVY ION COLLISIONS

In this section we will implement the $\delta f_{(2)}$ corrections in a 2+1 boost invariant hydrodynamic code. A full event-by-event simulation of heavy ion collisions with $\delta f_{(2)}$, together with a comparison to data, goes beyond the scope of this initial study. Nevertheless, the effect of $\delta f_{(2)}$ in larger simulations can be anticipated by understanding how the linear response is modified by $\delta f_{(2)}$. Indeed, the qualitative features of event-by-event hydrodynamic simulations of heavy ion collisions (including the correlations between the harmonics of different order) are reproduced by linear *and* quadratic response [8–10]. In central collisions the linear response is sufficient, and was recently used to produce one of the best estimates of the shear viscosity and its uncertainty to date [2]. We will calculate the linear response to a given deformation ϵ_n in order to estimate the influence of $\delta f_{(2)}$ on v_n .

In a given heavy ion event, the particle spectrum is expanded in harmonics

$$\frac{1}{p_T} \frac{dN}{dp_T d\phi_{\mathbf{p}}} = \frac{1}{2\pi p_T} \frac{dN}{dp_T} \left(1 + \sum_n v_n(p_T) e^{in(\phi_{\mathbf{p}} - \Psi_n(p_T))} + \text{complex conj.} \right) , \quad (3.1)$$

where $\phi_{\mathbf{p}}$ is the azimuthal angle around the beam pipe, and $v_n(p_T)$ are positive by definition. In a linear response approximation the n -th harmonic, $v_n(p_T)$, in the event is assumed to be proportional to the n -th cumulant, ϵ_n , which characterizes the deformation of the entropy distribution¹. Specifically, we first define the normalized entropy distribution at an time

¹ Note that we will use cumulants rather than moments to characterize the deformation [10, 13].

initial time τ_0

$$\rho(\mathbf{x}_\perp) \equiv \frac{\tau_0 s(\mathbf{x}_\perp)}{\int d^2x \tau_0 s(\mathbf{x}_\perp)}. \quad (3.2)$$

Writing the coordinates in the transverse plane $\mathbf{x}_\perp = (x, y)$ as a complex number, $z = x + iy = re^{i\phi}$, we define the first six cumulants characterizing the harmonic deformations of the initial distribution

$$\epsilon_1 e^{i\Phi_1} \equiv -\frac{\langle z^* z^2 \rangle}{\langle r^3 \rangle}, \quad (3.3a)$$

$$\epsilon_2 e^{i2\Phi_2} \equiv -\frac{\langle z^2 \rangle}{\langle r^2 \rangle}, \quad (3.3b)$$

$$\epsilon_3 e^{i3\Phi_3} \equiv -\frac{\langle z^3 \rangle}{\langle r^3 \rangle}, \quad (3.3c)$$

$$\epsilon_4 e^{i4\Phi_4} \equiv \frac{1}{\langle r^4 \rangle} \left[\langle z^4 \rangle - 3 \langle z^2 \rangle^2 \right], \quad (3.3d)$$

$$\epsilon_5 e^{i5\Phi_5} \equiv \frac{1}{\langle r^5 \rangle} \left[\langle z^5 \rangle - 10 \langle z^2 \rangle \langle z^3 \rangle \right], \quad (3.3e)$$

$$\epsilon_6 e^{i6\Phi_6} \equiv \frac{1}{\langle r^6 \rangle} \left[\langle z^6 \rangle - 15 \langle z^4 \rangle \langle z^2 \rangle - 10 \langle z^3 \rangle^2 + 30 \langle z^2 \rangle^3 \right], \quad (3.3f)$$

where $\langle \dots \rangle$ denote an average over $\rho(\mathbf{x}_\perp)$.

In a linear response approximation the orientation angle of n -th harmonic $\Psi_n(p_T)$ is aligned or anti-aligned with the cumulant angle Φ_n . Specifically, the spectrum in linear response is [13]

$$\frac{1}{p_T} \frac{dN}{dp_T d\phi_p} = \frac{1}{2\pi p_T} \frac{dN}{dp_T} \left(1 + 2 \sum_n w_n(p_T) \cos(n(\phi_p - \Phi_n)) + \dots \right). \quad (3.4)$$

Comparison with Eq. (3.1) shows that within this approximation scheme

$$v_n(p_T) = \sqrt{w_n^2(p_T)}, \quad (3.5)$$

and thus $w_n(p_T)$ differs at most by a sign from $v_n(p_T)$, *i.e.* $w_n(p_T) = v_n(p_T) \cos(n(\Psi_n(p_T) - \Phi_n))$. We will present the linear response coefficient, $w_n(p_T)/\epsilon_n$.

The linear response coefficient $w_n(p_T)/\epsilon_n$ is independent of many of the details of the initial state [13], and can be reasonably computed by initializing 2 + 1 boost invariant hydrodynamics with a deformed Gaussian distribution, where the rms radius and amplitude of the Gaussian are adjusted to match the rms radius and total entropy of the event. For example, to simulate w_3 at RHIC at an impact parameter of $b = 7.45$ fm we initialize a Gaussian deformed by $\epsilon_3 = 0.05$ with $\Phi_3 = 0$

$$\tau_0 s(\mathbf{x}, \tau_0) = C_s \langle N_p \rangle \left[1 + \frac{\langle r^3 \rangle \epsilon_3}{24} \left(\left(\frac{\partial}{\partial x} \right)^3 - 3 \left(\frac{\partial}{\partial y} \right)^2 \frac{\partial}{\partial x} \right) \right] \frac{e^{-\frac{r^2}{\langle r^2 \rangle}}}{\pi \langle r^2 \rangle}, \quad (3.6)$$

where C_s sets the total multiplicity in the event. Here $\langle r^2 \rangle$ and $\langle N_p \rangle$ are computed using the Phobos Glauber model [14]. In order that the total entropy closely matches the total

Momentum Dependence	$\eta\tau_\pi$	λ_1
Linear Ansatz ($\alpha = 1$)	$(d + 1) = 5$	$(d + 1)^2/(d + 3) = 25/7$
Quadratic Ansatz ($\alpha = 0$)	$(d + 2) = 6$	$(d + 2) = 6$

TABLE I. A compilation of rescaled second order transport coefficients for a linear and quadratic ansatz in a relaxation time approximation for classical statistics [4]. All numbers in this table should be *multiplied* by $\eta^2/(e + \mathcal{P})$. In a relaxation time approximation $\lambda_2 = -2\eta\tau_\pi$ and $\lambda_3 = 0$ [4].

entropy in more complete simulations [5, 15], we take $C_s = 15.9$ and 28.04 at RHIC and LHC respectively. This procedure has been used previously by the authors to determine the linear and non-linear response [10, 11, 13].

After initializing the Gaussian, we evolve the system with second order hydrodynamics, Eq. (2.4) and Eq. (2.8), using a variant of the central scheme developed previously [16, 17]. Then for a given n -th order harmonic perturbation ϵ_n we compute w_n/ϵ_n by performing the freezeout integral at a constant temperature. This evolution requires an equation of state and specified hydrodynamic parameters at first and second order. In what follows we will consider a conformal equation of state for a single component classical gas, and a lattice motivated equation of state previously used by Romatschke and Luzum [5].

Since it is only for the conformal equation of state $p = \frac{1}{3}\epsilon$ that the analysis of Section II is strictly valid we will discuss this case first, and then discuss the necessary modifications for a lattice based equation of state. To keep the final freezeout volume of the conformal equation of state approximately equal to the much more realistic lattice based equation of state, we choose the final freezeout temperature ($T_{\text{fo}} = 96$ MeV) so that the entropy density at freezeout $s_{\text{frz}} = 1.87 \text{ fm}^{-3}$ equals the entropy density of a hadron resonance gas at a temperature of $T = 150$ MeV. The relation between the temperature and energy density for the conformal equation of state is $e/T^4 = 12.2$, which is the value for a two flavor ideal quark-gluon plasma. The motivation for these choices, the parameters of the conformal equation of state, and further details about the initial conditions and freezeout we refer to our previous work – see especially Appendix B of Ref. [13].

The second order transport coefficients $\eta\tau_\pi$ and λ_1 are all constrained by the momentum dependence of the relaxation time and the shear viscosity through Eqs. (2.23), (2.28), (2.29). As discussed in Ref. [7], there are two limits for this momentum dependence which span the gamut of reasonable possibilities. In the first limit the relaxation time grows linearly with momentum, and $\alpha = 0$ in Eq. (2.12). This is known as the *quadratic ansatz*, and is most often used to simulate heavy ion collisions. In a similarly extreme limit the relaxation time is independent of momentum, and $\alpha = 1$ in Eq. (2.12). This is known as the *linear ansatz*, and this limit provides a useful foil to the more commonly adopted quadratic ansatz. Once the shear viscosity and the momentum dependence of the relaxation time are given, the collision kernel is completely specified in the relaxation time approximation, and all transport coefficients are fixed. For a linear and quadratic ansatz we record the appropriate second order transport coefficients in Table I.

So far this section has detailed the initial and freezeout conditions, as well as the second

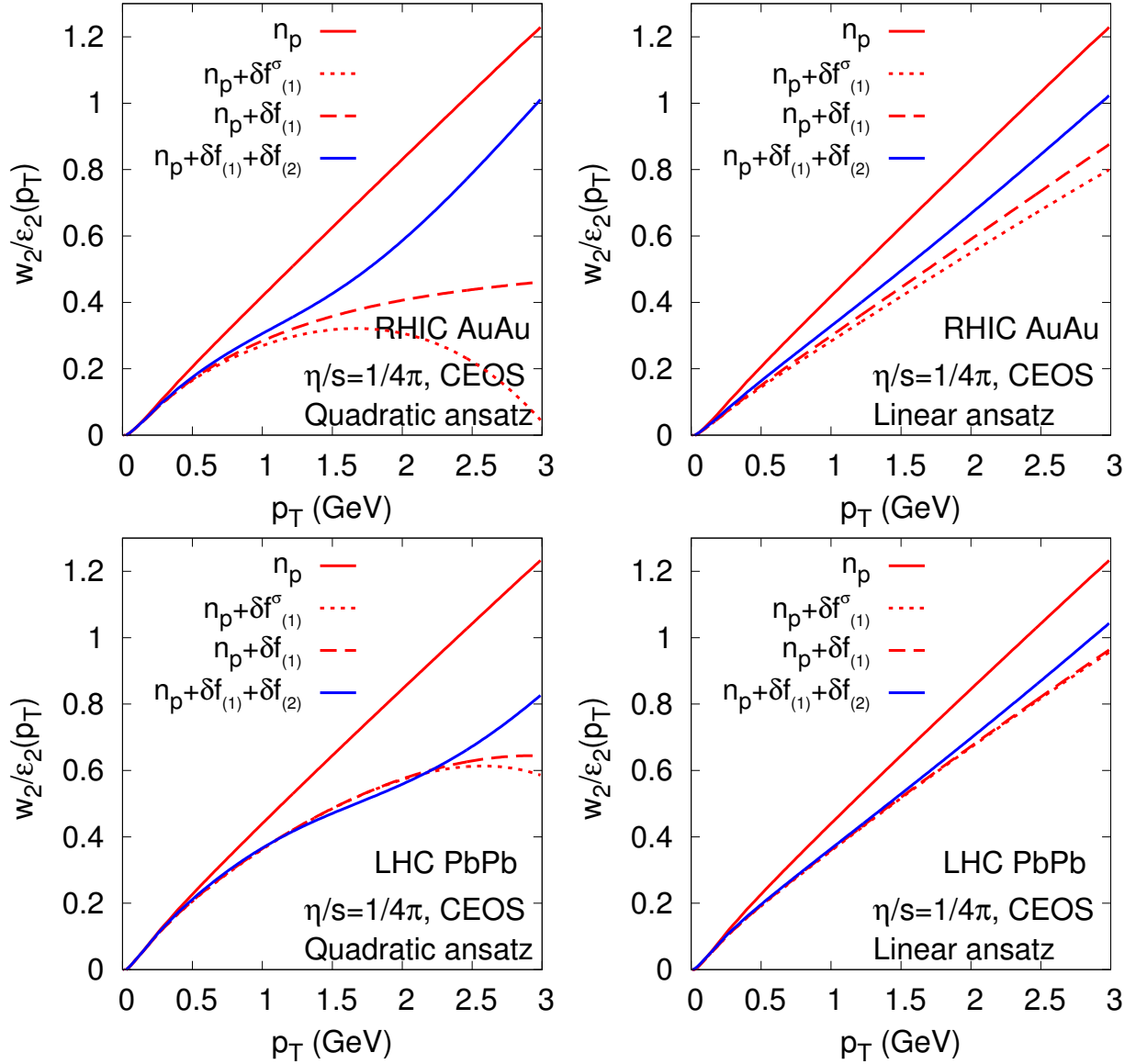


FIG. 1. Differential $w_2(p_T)/\epsilon_2$ for RHIC and LHC initial conditions, for a linear and quadratic ansatz, and a conformal equation of state (CEOS). The n_p curves show the flow from second order hydrodynamics without the viscous correction to the distribution function; $\delta f_{(1)}$ and $\delta f_{(1)} + \delta f_{(2)}$ show the flow with the viscous correction at first and second order; and finally, the $\delta f_{(1)}^\sigma$ result uses $-\eta\sigma^{\mu\nu}$ instead of $\pi^{\mu\nu}$ in the first order result (see Eq. (2.17)). The freezeout temperature is chosen so that the freezeout entropy density of the conformal gas equals that of a hadronic resonance gas at a temperature of $T = 150$ MeV.

order parameters which are used in the conformal equation of state. Fig. 1 shows the resulting elliptic flow for the quadratic and linear ansätze for a conformal equation of state including the first and second order δf . A conformal equation of state has a strong expansion, and, as a result, generally over estimates the magnitude of the δf correction. Thus the conformal analysis provides a schematic upper bound on the magnitude of the $\delta f_{(2)}$ correction. Further discussion of these results is reserved for Section IV

Strictly speaking the analysis of Section II is useful only for a single component conformal gas. Nevertheless, we believe the usefulness of the analysis extends beyond this limited regime [4]. Indeed, examining the steps in the derivation one finds that only very-few non conformal terms appear at each order. For instance, if non-conformal corrections are kept in Eq. (2.17) one finds

$$\delta f_{(1)-\text{non-conf}}^\sigma(\mathbf{p}) = \mathcal{C}_p n'_p \left[\frac{P^\mu P^\nu \sigma_{\mu\nu}}{2T^3} + \left(-\frac{E_{\mathbf{p}}^2 - p^2}{3T^3} + \frac{(\frac{1}{3} - c_s^2)E_{\mathbf{p}}^2}{T^3} \right) \nabla_\mu U^\mu \right], \quad (3.7)$$

which shows that non-conformal terms (the second term in Eq. (3.7)) are either suppressed by $\frac{1}{3} - c_s^2$, or are suppressed at high momentum relative to the conformal terms.

To extend our analysis to a multi-component non-conformal equation of state we have followed the simplified treatment that is used in almost all simulations of heavy ion collisions. First, we will treat all species independently

$$P^\mu \partial_\mu f_{\mathbf{p}}^a(X) = -\frac{T^2}{\mathcal{C}_p^a} [f_{\mathbf{p}}^a(X) - n^a(-P \cdot U_*(X)/T_*(X))] , \quad (3.8)$$

where $a = \pi, K, \rho, \dots$ is a species label². We will also adopt the quadratic ansatz $\alpha = 0$, so that \mathcal{C}_p^a is independent of momentum. Then for every species we define the partial entropy and shear viscosity as in Eqs. 2.23 and 2.25

$$\eta_a = \frac{-\mathcal{C}_p^a}{(d-1)(d+1)} \left[\frac{g_a}{T^3} \int_{\mathbf{p}} n_p^{a'} \frac{p^4}{E_p} \right], \quad (3.9a)$$

$$s_a = \frac{-1}{(d-1)} \left[\frac{g_a}{T^2} \int_{\mathbf{p}} n_p^{a'} p^2 \right], \quad (3.9b)$$

where g_a is the spin-isospin degeneracy factor. The full shear viscosity and entropy density is a sum of the partial results, $\eta = \sum_a \eta_a$ and $s = \sum_a s_a$. We require that η_a/s_a is equal to η/s for each species, and thus the relaxation time parameter \mathcal{C}_p^a is, in principle, different for each species. However, for a classical gas the two integrals in square brackets are equal upon integrating by parts, and thus $\mathcal{C}_p^a = \eta_a/s_a = \eta/s$ is independent of the mass and species label. For fermi-dirac and bose statistics these integrals are very nearly equal (to 4% accuracy) for all values of the mass, and \mathcal{C}_p^a is approximately equal to η/s for all species independent of mass and statistics.

Now that the relaxation time parameter \mathcal{C}_p^a is fixed for each species, the corresponding second order δf for each species is found by appending a species label, $n_p \rightarrow n_p^a$ and $\mathcal{C}_p \rightarrow \mathcal{C}_p^a$, to previous results. For a multi-component gas with a quadratic ansatz we find

$$\eta\tau_\pi + \lambda_1 = \sum_a (\mathcal{C}_p^a)^2 \left[\frac{2g_a}{(d-1)(d+1)(d+3)T^6} \int_{\mathbf{p}} n_p^{a''} \frac{p^6}{E_p} \right], \quad (3.10a)$$

$$\eta\tau_\pi = \sum_a (\mathcal{C}_p^a)^2 \left[\frac{-g_a}{(d-1)(d+1)T^5} \int_{\mathbf{p}} n_p^{a'} p^4 \right]. \quad (3.10b)$$

² There have been several efforts to go beyond this extreme species independent approximation [7, 18].

For classical statistics $\mathcal{C}_p^a = \eta/s$, and integrating the first integral in square brackets by parts yields a simple relation noted previously [4]

$$\lambda_1 = \eta\tau_\pi \quad (\text{for } \alpha = 0). \quad (3.11)$$

The remaining thermodynamic integrals are most easily done numerically; summing over all hadronic species with mass less than 1.5 GeV we find

$$\lambda_1 = \eta\tau_\pi = \frac{\eta^2}{(e + \mathcal{P})} 8.9. \quad (3.12)$$

Thus, $T\tau_\pi/(\eta/s) = 8.9$ would seem to be the most consistent value for the 2nd order transport coefficients during the hydrodynamic evolution of the hadronic phase. However, this value for $T\tau_\pi$ is somewhat too large to be used comfortably in the simulation [19]. Further, $T\tau_\pi$ decreases as temperature increases, and $T\tau_\pi/(\eta/s) \simeq 5$ is good approximation in the QGP phase [4]. We have therefore taken $\lambda_1 = \eta\tau_\pi = 5\eta^2/(e + \mathcal{P})$ throughout the evolution. This means that there is a small inconsistency between the second order δf at freezeout, and the second order parameters used to simulate the bulk of the hydrodynamic evolution. Similar inconsistencies are found in all attempts to consistently couple hydrodynamic codes with hadronic cascades [20].

To summarize, in this section we have specified precisely the initial conditions, the equation of state, the transport coefficients at first and second order, and the first and second order corrections to the distribution functions. We have used this setup to compute the linear response coefficients w_n/ϵ_n for RHIC and LHC initial conditions for the first six harmonics. Our results are displayed in Fig. 2 and Fig. 3. We will discuss the physics of these curves in the next section.

IV. DISCUSSION

This work computed the second order viscous correction to the thermal distribution function, $\delta f_{(2)}$, and used this result to estimate the effect of second order corrections on the harmonic spectrum. Our principle results are shown in Fig. 1 for a conformal equation of state, and Fig. 2, and Fig. 3 for a lattice based equation of state. First, examine the v_2 curves for the conformal EOS shown in Fig. 1. The most important remark is that even for a conformal equation of state, where the expansion is most violent, the derivative expansion converges acceptably for $p_T \lesssim 1.5$ GeV, *i.e.* the second order correction is small compared to the first order correction. Not surprisingly, when a linear ansatz is used for δf (rather than the more popular quadratic ansatz) the convergence of the derivative expansion is improved at high p_T . Typically in hydrodynamic simulations of heavy ion collisions, the strictly first order $\delta f_{(1)}^\sigma$ is replaced by the $\delta f_{(1)}$ which incorporates some, but not all, second order terms³. Examining Fig. 1, and also Fig. 2 and Fig. 3, we see that, while the sign of the second order correction is correctly reproduced by this incomplete treatment, the magnitude of the correction is generally significantly underestimated, and the p_T dependence of the second order correction is qualitatively wrong.

³ As discussed above, $\delta f_{(1)}$ uses $\pi^{\mu\nu}$ in place of $-\eta\sigma^{\mu\nu}$ when calculating the first order correction.

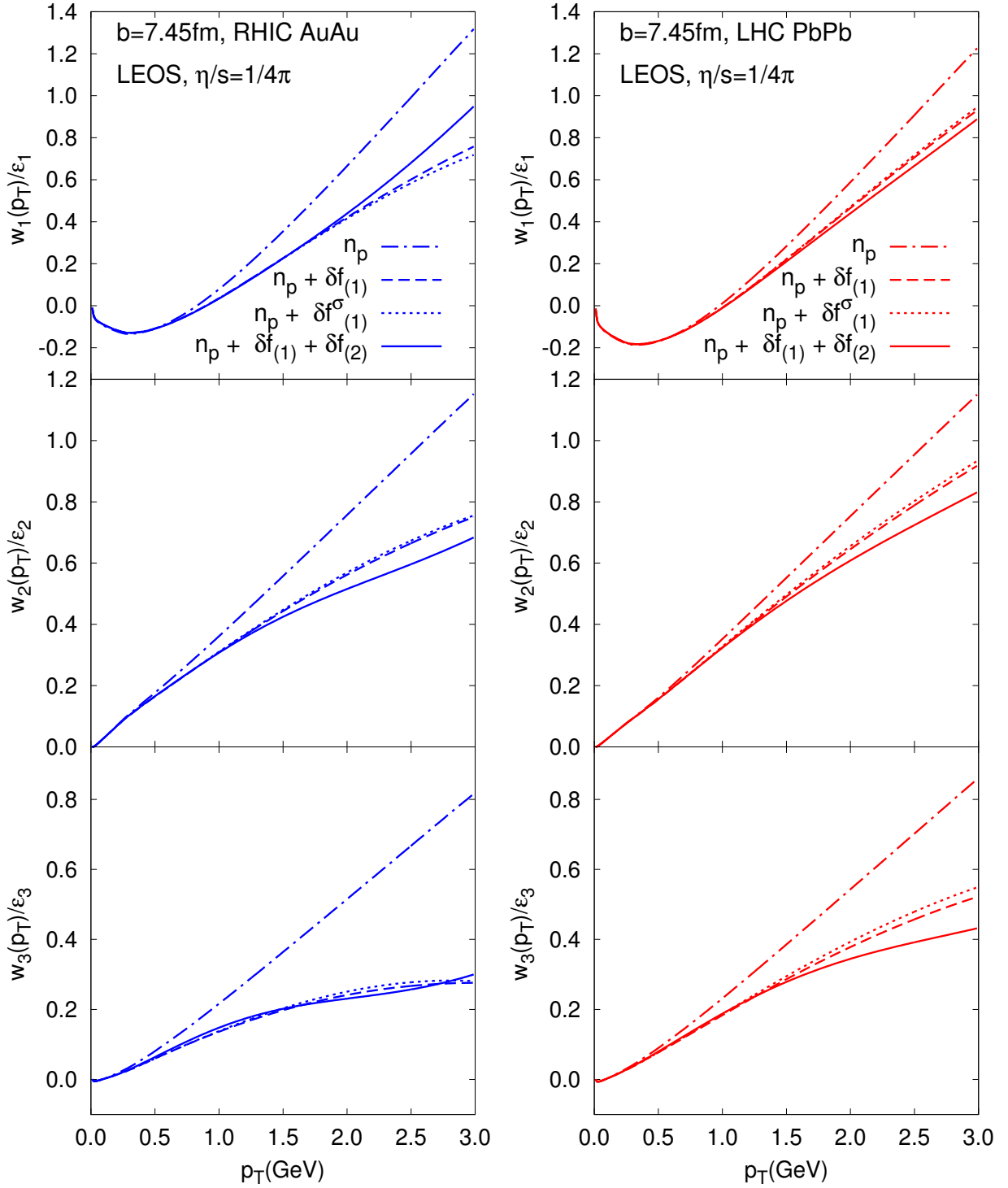


FIG. 2. Differential w_n/ϵ_n from various viscous hydrodynamic simulations at $b = 7.45$ fm for RHIC and LHC initial conditions, and a lattice equation of state (LEOS) with $T_0 = 150$ MeV. Here the n_p curve shows the flow from second order hydrodynamics without the viscous correction to the distribution function; $\delta f_{(1)}$ and $\delta f_{(1)} + \delta f_{(2)}$ show the flow with the viscous correction at first and second order respectively; and finally, the $\delta f_{(1)}^\sigma$ curve uses $-\eta\sigma^{\mu\nu}$ instead of $\pi^{\mu\nu}$ in the first order viscous correction (see Eq. (2.17)).

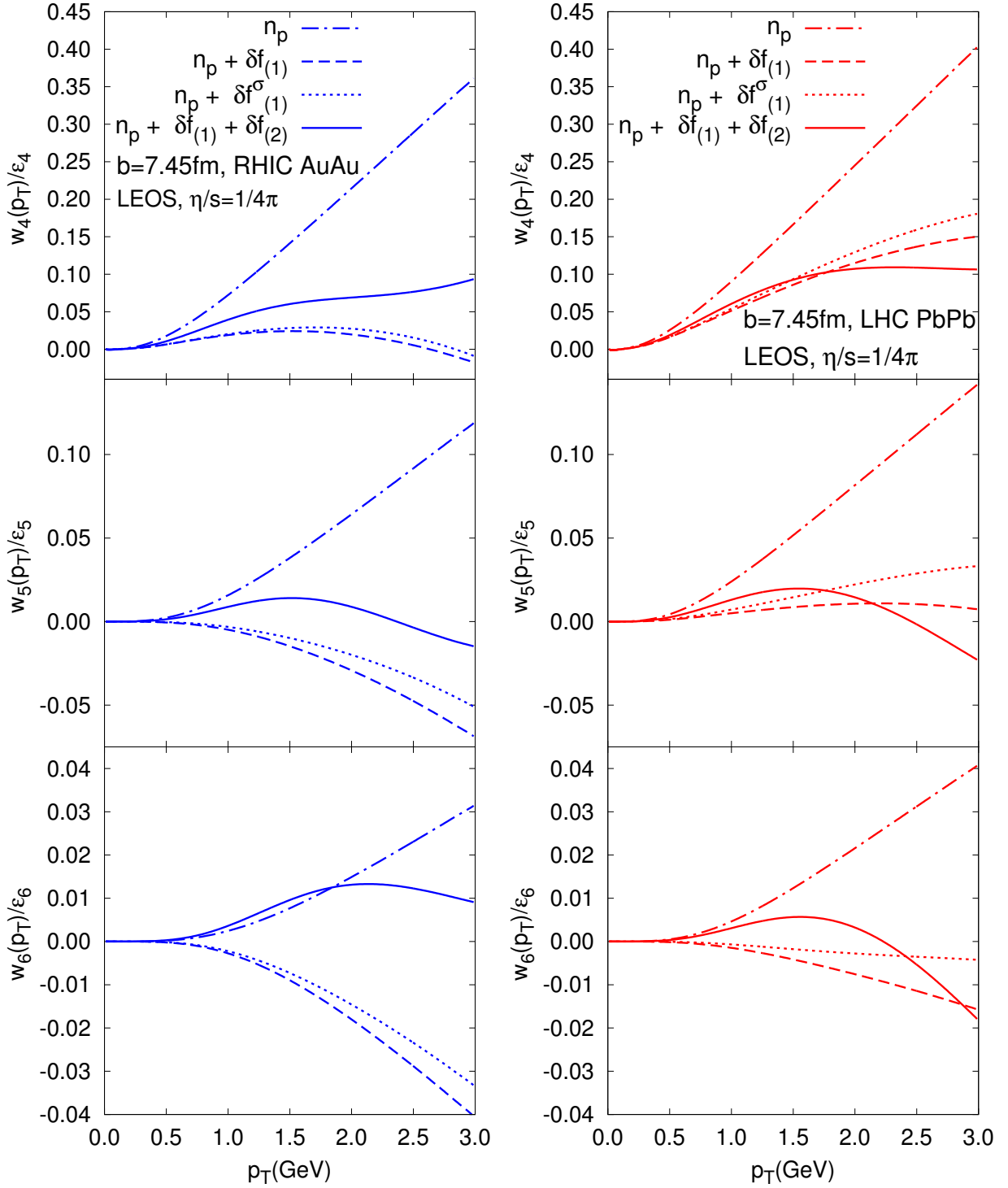


FIG. 3. Differential w_n/ϵ_n from various viscous hydrodynamic simulations at $b = 7.45$ fm for RHIC and LHC initial conditions, and a lattice equation of state (LEOS) with $T_{fo} = 150$ MeV. Here the n_p curve shows the flow from second order hydrodynamics without the viscous correction to the distribution function; $\delta f_{(1)}$ and $\delta f_{(1)} + \delta f_{(2)}$ show the flow with the viscous correction at first and second order respectively; and finally, the $\delta f_{(1)}^\sigma$ curve uses $-\eta\sigma^{\mu\nu}$ instead of $\pi^{\mu\nu}$ in the first order viscous correction (see Eq. (2.17)).

Most of these observations remain true for the more realistic lattice equation of state shown in Fig. 2 and Fig. 3. Generally, second order corrections are quite small for the first three harmonics, v_1 to v_3 , and become increasingly important as the harmonic number increases. Indeed, for v_6 at RHIC and the LHC, the second order viscous correction is of order one, and the hydrodynamic estimate can no longer be trusted. It is also instructive to note that the sign of the second order viscous correction for $p_T \lesssim 1.5 \text{ GeV}$ is positive, *i.e.* second order corrections bring the $v_n(p_T)$ curves closer to the ideal results. Generally, when the first order correction, becomes so large as to make w_n negative⁴, the second order correction conspires to keep w_n positive. When constraining η/s with hydrodynamic simulations, the second order corrections are most important for v_4 and v_5 . Indeed, at RHIC these corrections are quite important for v_5 even in central collisions.

For a practical perspective, using $\delta f_{(2)}$ in a hydrodynamic simulation is not particularly more difficult than using $\delta f_{(1)}$, and Eq. 2.18 can be readily implemented in most hydro codes. The functional form of $\delta f_{(2)}$ and its magnitude is about as well constrained as $\delta f_{(1)}$, and consistency with the second order hydrodynamic evolution would seem to mandate its use. At very least $\delta f_{(2)}$ should be taken into consideration when estimating the uncertainty in the η/s extracted from heavy ion collisions. Finally, when trying to use hydrodynamics in very small systems such as proton-nucleus collisions at RHIC and the LHC [21–27], second order corrections to δf should be used in order to monitor the convergence of the gradient expansion.

Acknowledgments:

We thank Ulrich Heinz for emphasizing that v_n is positive by definition. D. Teaney is a RIKEN-RBRC fellow. This work was supported in part by the Sloan Foundation and by the Department of Energy, DE-FG-02-08ER4154.

Appendix A: Tensor decomposition of $\delta f_{(2)}$

The goal of this appendix is to compute $\delta f_{(2)}$ and to record how this results transforms under rotations in the local rest frame. Our starting point is Eqs. (2.18) which we rewrite in terms of irreducible tensors under rotations in the local rest frame.

A systematic strategy decomposes all derivatives into temporal and spatial components

$$\partial_\mu = -U_\mu D + \nabla_\mu, \quad (\text{A1})$$

where the spatial component ∇_μ is orthogonal to U_μ . When differentiating a quantity that is already first order (*i.e.* $P^\mu \partial_\mu \delta f_{(1)}^\sigma$), we can use the lowest order conformal equations of motion to rewrite time derivatives in terms of spatial derivatives

$$D \ln T = -c_s^2 \nabla \cdot U, \quad (\text{A2})$$

$$DU_\mu = -\nabla_\mu \ln T, \quad (\text{A3})$$

⁴ v_n is positive by definition, see Eq. (3.1). Negative values of w_n indicate that the flow angle $\Psi_n(p_T)$ is anti-aligned with the participant angle plane, Φ_n .

where $c_s^2 = (e + \mathcal{P})/(Tc_v) = 1/(d-1)$. Finally, the resulting tensors can be decomposed into symmetric, traceless, and spatial tensors as in Eq. (2.2), which transform irreducibly under rotations in the local rest frame. To illustrate the procedure, we record the decomposition of $D\sigma_{\alpha\beta}$

$$D\sigma_{\alpha\beta} = D(\sigma^{\mu\nu}\Delta_{\mu\alpha}\Delta_{\nu\beta}) = \Delta_{\mu\alpha}\Delta_{\nu\beta}D\sigma^{\mu\nu} + \sigma^{\mu\nu}D(\Delta_{\mu\alpha}\Delta_{\nu\beta}), \quad (\text{A4})$$

$$= \langle D\sigma_{\alpha\beta} \rangle - (\sigma_{\beta}^{\mu}u_{\alpha}\nabla_{\mu}\ln T + u_{\beta}\sigma_{\alpha}^{\nu}\nabla_{\nu}\ln T). \quad (\text{A5})$$

Similarly, the symmetrized spatial tensor $\{\nabla_{\mu}\sigma_{\alpha\beta}\}_{\text{sym}}$ that arises when differentiating $\delta f_{(1)}^{\sigma}$ is decomposed as

$$\begin{aligned} \{\nabla_{\mu}\sigma_{\alpha\beta}\}_{\text{sym}} = & \langle \nabla_{\mu}\sigma_{\alpha\beta} \rangle + \left\{ \frac{2}{d+1}\Delta_{\mu\alpha}\nabla_{\gamma}\sigma_{\beta}^{\gamma} + u_{\alpha}\langle \sigma_{\beta}^{\rho}\sigma_{\mu\rho} \rangle \right. \\ & \left. + u_{\alpha}\frac{\Delta_{\mu\beta}}{d-1}\sigma^2 + 2u_{\alpha}\langle \sigma_{\beta}^{\rho}\Omega_{\mu\rho} \rangle + 2u_{\alpha}\frac{\sigma_{\mu\beta}}{d-1}\nabla \cdot U \right\}_{\text{sym}}, \end{aligned} \quad (\text{A6})$$

where we have used

$$\nabla_{\mu}u_{\rho} = \frac{1}{2}\sigma_{\mu\rho} + \Omega_{\mu\rho} + \frac{\Delta_{\mu\rho}}{d-1}\nabla \cdot U. \quad (\text{A7})$$

Finally, we note that

$$\langle \partial_{\lambda}\pi_{\mu}^{\lambda} \rangle = \Delta_{\mu\lambda_2}\partial_{\lambda_1}\pi^{\lambda_1\lambda_2} = -\eta \left[(d-2)\langle \sigma_{\mu\lambda}\nabla^{\lambda}\ln T \rangle + \langle \nabla_{\lambda}\sigma_{\mu}^{\lambda} \rangle \right], \quad (\text{A8})$$

where we have used the first order expression, $\pi^{\mu\nu} = -\eta\sigma^{\mu\nu}$, the conformal temperature dependence of $\eta \propto T^{d-1}$, and the lowest order equations of motion.

With this automated set of steps, we start with Eq. (2.18) and place $\delta f_{(2)}^{\sigma}$ into its canonical form

$$\begin{aligned} \delta f_{(2)}^{\sigma} = & \chi_{1p} \frac{P^{\mu_1}P^{\mu_2}P^{\mu_3}P^{\mu_4}}{T^6} \langle \sigma_{\mu_1\mu_2}\sigma_{\mu_3\mu_4} \rangle + \chi_{2p} \frac{P^{\mu_1}P^{\mu_2}P^{\mu_3}}{T^5} [\langle \nabla_{\mu_1}\sigma_{\mu_2\mu_3} \rangle - 3\langle \sigma_{\mu_1\mu_2}\nabla_{\mu_3}\ln T \rangle] \\ & + \left(\chi_{1p}\frac{4\bar{p}^2}{d+3} - \chi_{2p}\bar{E}_p \right) \frac{P^{\mu_2}P^{\mu_1}}{T^4} \langle \sigma_{\mu_2}^{\lambda}\sigma_{\mu_1\lambda} \rangle \\ & + \chi_{2p}\bar{E}_p \frac{P^{\mu_2}P^{\mu_1}}{T^4} \left[\langle D\sigma_{\mu_2\mu_1} \rangle + \frac{\sigma_{\mu_2\mu_1}}{d-1}\nabla \cdot U - 2\langle \sigma_{\mu_2}^{\lambda}\Omega_{\mu_1\lambda} \rangle \right] \\ & + \xi_{3p} \frac{P^{\mu_2}}{T^3} \left[-\langle \nabla_{\lambda}\sigma_{\mu_2}^{\lambda} \rangle - (d-2)\langle \sigma_{\mu_2\lambda}\nabla^{\lambda}\ln T \rangle \right] + \frac{\xi_{4p}}{T^2}\sigma^2, \end{aligned} \quad (\text{A9})$$

where the functions χ_{0p} , χ_{1p} , χ_{2p} and ξ_{3p} and ξ_{4p} are recorded in the text, Eq. (2.31).

In this form it is easy to integrate over the the phase space to determine the viscous stress

$$\pi^{\mu\nu} = \pi_{(1)}^{\mu\nu} + \pi_{(2)}^{\mu\nu} = \int_p \frac{P^{\mu}P^{\nu}}{P^0} (\delta f_{(1)}^{\sigma} + \delta f_{(2)}^{\sigma}), \quad (\text{A10})$$

where $\pi_{(1)}^{\mu\nu}$ and $\pi_{(2)}^{\mu\nu}$ are given by static form of the constituent relation Eq. (2.5). Rotational invariance in the rest frame reduces these tensor integrals, *e.g.*

$$\int_p \chi_{0p} \frac{P^{\mu_1}P^{\mu_2}P^{\mu_3}P^{\mu_4}}{P^0} \langle O_{\mu_3\mu_3} \rangle = \left[\frac{2}{(d-1)(d+1)} \int_p \chi_{0p} \frac{p^4}{E_p} \right] \langle O^{\mu_1\mu_2} \rangle, \quad (\text{A11})$$

yielding the equations for the transport coefficients written in the text, Eqs. (2.23), (2.28), and (2.29). In addition, we see that independent of the collision integral one finds the kinetic theory expectations identified in Ref. [4]

$$\lambda_2 = -2\eta\tau_\pi, \quad \text{and} \quad \lambda_3 = 0. \quad (\text{A12})$$

Finally, in presenting these results in the text, and in implementing the results in a realistic hydrodynamic simulation, we have used the dynamic form of second order hydrodynamics, where $\pi^{\mu\nu}$ is treated as a dynamic variable. This choice amounts to using $-\pi_{\mu\nu}/\eta$ in place of $\sigma_{\mu\nu}$. In $\delta f_{(2)}^\sigma$ this reparametrizations yields the replacements:

$$\langle D\sigma_{\mu_1\mu_2} \rangle + \frac{\sigma_{\mu_1\mu_2}}{d-1} \nabla \cdot U - 2 \langle \sigma_{\mu_1}^\lambda \Omega_{\mu_2\lambda} \rangle \rightarrow \frac{1}{\eta\tau_\pi} [\pi_{\mu_1\mu_2} + \eta\sigma_{\mu_1\mu_2}] - \frac{\lambda_1}{\eta\tau_\pi} \frac{1}{\eta^2} \langle \pi_{\mu_1}^\lambda \pi_{\mu_2\lambda} \rangle, \quad (\text{A13})$$

$$\langle \nabla_{\mu_1} \sigma_{\mu_2\mu_3} \rangle - 3 \langle \sigma_{\mu_1\mu_2} \nabla_{\mu_3} \ln T \rangle \rightarrow \frac{1}{\eta} [(d+2) \langle \pi_{\mu_1\mu_2} \nabla_{\mu_3} \ln T \rangle - \langle \nabla_{\mu_1} \pi_{\mu_2\mu_3} \rangle], \quad (\text{A14})$$

and Eq. (A8). In addition, when replacing $\sigma_{\mu\nu}$ with $-\pi_{\mu\nu}/\eta$ in the first order result, the difference $\frac{1}{\eta}(\pi_{\mu\nu} + \eta\sigma_{\mu\nu})$ must be appended to the second order result – see Eq. (2.19). The full result for $\delta f_{(1)}$ and $\delta f_{(2)}$ is given in Eqs. (2.20) and (2.30) respectively.

-
- [1] For an up to date review, see: Ulrich W Heinz and Raimond Snellings, “Collective flow and viscosity in relativistic heavy-ion collisions,” (2013), [arXiv:1301.2826 \[nucl-th\]](#).
 - [2] Matthew Luzum and Jean-Yves Ollitrault, “Extracting the shear viscosity of the quark-gluon plasma from flow in ultra-central heavy-ion collisions,” Nucl.Phys.A (2012), [arXiv:1210.6010 \[nucl-th\]](#).
 - [3] Rudolf Baier, Paul Romatschke, Dam Thanh Son, Andrei O. Starinets, and Mikhail A. Stephanov, “Relativistic viscous hydrodynamics, conformal invariance, and holography,” JHEP **0804**, 100 (2008), [arXiv:0712.2451 \[hep-th\]](#).
 - [4] Mark Abraao York and Guy D. Moore, “Second order hydrodynamic coefficients from kinetic theory,” Phys.Rev. **D79**, 054011 (2009), [arXiv:0811.0729 \[hep-ph\]](#).
 - [5] Matthew Luzum and Paul Romatschke, “Conformal Relativistic Viscous Hydrodynamics: Applications to RHIC results at $\sqrt{s} = 200$ GeV,” Phys. Rev. **C78**, 034915 (2008), [arXiv:0804.4015 \[nucl-th\]](#).
 - [6] See for example: Derek A. Teaney, “Viscous Hydrodynamics and the Quark Gluon Plasma,” (2009), invited review for ‘Quark Gluon Plasma 4’. Editors: R.C. Hwa and X.N. Wang, World Scientific, Singapore., [arXiv:0905.2433 \[nucl-th\]](#).
 - [7] Kevin Dusling, Guy D. Moore, and Derek Teaney, “Radiative energy loss and v(2) spectra for viscous hydrodynamics,” Phys.Rev. **C81**, 034907 (2010), [arXiv:0909.0754 \[nucl-th\]](#).
 - [8] Zhi Qiu and Ulrich W. Heinz, “Event-by-event shape and flow fluctuations of relativistic heavy-ion collision fireballs,” Phys.Rev. **C84**, 024911 (2011), [arXiv:1104.0650 \[nucl-th\]](#).

- [9] Fernando G. Gardim, Frederique Grassi, Matthew Luzum, and Jean-Yves Ollitrault, “Mapping the hydrodynamic response to the initial geometry in heavy-ion collisions,” *Phys.Rev.* **C85**, 024908 (2012), [arXiv:1111.6538 \[nucl-th\]](#).
- [10] Derek Teaney and Li Yan, “Non linearities in the harmonic spectrum of heavy ion collisions with ideal and viscous hydrodynamics,” *Phys.Rev.* **C86**, 044908 (2012), [arXiv:1206.1905 \[nucl-th\]](#).
- [11] Derek Teaney and Li Yan, “Non-linear flow response and reaction plane correlations,” (2012), [arXiv:1210.5026 \[nucl-th\]](#).
- [12] Derek Teaney, “Finite temperature spectral densities of momentum and R-charge correlators in N=4 Yang Mills theory,” *Phys.Rev.* **D74**, 045025 (2006), [arXiv:hep-ph/0602044 \[hep-ph\]](#).
- [13] Derek Teaney and Li Yan, “Triangularity and Dipole Asymmetry in Heavy Ion Collisions,” *Phys.Rev.* **C83**, 064904 (2011), [arXiv:1010.1876 \[nucl-th\]](#).
- [14] B. Alver, M. Baker, C. Loizides, and P. Steinberg, “The PHOBOS Glauber Monte Carlo,” (2008), [arXiv:0805.4411 \[nucl-ex\]](#).
- [15] Matthew Luzum, “Elliptic flow at energies available at the CERN Large Hadron Collider: Comparing heavy-ion data to viscous hydrodynamic predictions,” *Phys.Rev.* **C83**, 044911 (2011), [arXiv:1011.5173 \[nucl-th\]](#).
- [16] L. Pareschi, “Central differencing based numerical schemes for hyperbolic conservation laws with relaxation terms,” *SIAM Journal on Numerical Analysis* **39**, 1395–1417 (2001), <http://epubs.siam.org/doi/pdf/10.1137/S0036142900375906>.
- [17] K. Dusling and D. Teaney, “Simulating elliptic flow with viscous hydrodynamics,” *Phys.Rev.* **C77**, 034905 (2008), [arXiv:0710.5932 \[nucl-th\]](#).
- [18] G.S. Denicol and H. Niemi, “Derivation of transient relativistic fluid dynamics from the Boltzmann equation for a multi-component system,” (2012), [arXiv:1212.1473 \[nucl-th\]](#).
- [19] See for example: Huichao Song and Ulrich W. Heinz, “Causal viscous hydrodynamics in 2+1 dimensions for relativistic heavy-ion collisions,” *Phys.Rev.* **C77**, 064901 (2008), [arXiv:0712.3715 \[nucl-th\]](#).
- [20] Huichao Song, Steffen A. Bass, Ulrich Heinz, Tetsufumi Hirano, and Chun Shen, “Hadron spectra and elliptic flow for 200 A GeV Au+Au collisions from viscous hydrodynamics coupled to a Boltzmann cascade,” *Phys.Rev.* **C83**, 054910 (2011), [arXiv:1101.4638 \[nucl-th\]](#).
- [21] Serguei Chatrchyan *et al.* (CMS Collaboration), “Observation of long-range near-side angular correlations in proton-lead collisions at the LHC,” *Phys.Lett.* **B718**, 795–814 (2013), [arXiv:1210.5482 \[nucl-ex\]](#).
- [22] Betty Abelev *et al.* (ALICE Collaboration), “Long-range angular correlations on the near and away side in p-Pb collisions at $\sqrt{s_{NN}} = 5.02$ TeV,” *Phys.Lett.* **B719**, 29–41 (2013), [arXiv:1212.2001 \[nucl-ex\]](#).
- [23] Georges Aad *et al.* (ATLAS Collaboration), “Observation of Associated Near-side and Away-

- side Long-range Correlations in $\sqrt{s_{NN}} = 5.02$ TeV Proton-lead Collisions with the ATLAS Detector,” (2012), [arXiv:1212.5198 \[hep-ex\]](#).
- [24] Piotr Bozek and Wojciech Broniowski, “Correlations from hydrodynamic flow in p-Pb collisions,” *Phys.Lett. B* **718**, 1557–1561 (2013), [arXiv:1211.0845 \[nucl-th\]](#).
- [25] A. Adare *et al.* (PHENIX Collaboration), “Quadrupole anisotropy in dihadron azimuthal correlations in central d+Au collisions at $\sqrt{s_{NN}} = 200$ GeV,” (2013), [arXiv:1303.1794 \[nucl-ex\]](#).
- [26] Edward Shuryak and Ismail Zahed, “High Multiplicity pp and pA Collisions: Hydrodynamics at its Edge and Stringy Black Hole,” (2013), [arXiv:1301.4470 \[hep-ph\]](#).
- [27] Adam Bzdak, Bjoern Schenke, Prithwish Tribedy, and Raju Venugopalan, “Initial state geometry and the role of hydrodynamics in proton-proton, proton-nucleus and deuteron-nucleus collisions,” (2013), [arXiv:1304.3403 \[nucl-th\]](#).